

Eulerian-Style Measurements Incorporating Mechanical Sensors

Chapter Outline

| | | | |
|---|------------|--|------------|
| 8.1. Eulerian-Style Measurements | 242 | 8.6. Calibration of Current Meters | 255 |
| 8.2. Savonius Rotor Current Meters | 242 | 8.7. Graphical Methods of Displaying Ocean Current Measurements | 258 |
| 8.3. Savonius Rotor and Miniature Vane Vector-Averaging Current Meters | 249 | 8.8. Advantages and Limitations of Mechanical Sensors | 263 |
| 8.4. Propeller Rotor Current Meter (Plessey Current Meter) | 250 | References | 263 |
| 8.5. Biaxial Dual Orthogonal Propeller Vector-Measuring Current Meters | 253 | Bibliography | 264 |

With the growing dependence of man on the oceans, the need to acquire knowledge of ocean currents has also correspondingly increased. Ocean-current measurements are made in many ways. One such method is the so-called *Eulerian method*, in which flow of water in the ocean (i.e., ocean current) past a geographically fixed position is determined as a function of time using a single instrument or a chain of instruments deployed at a specific station. Current measurements in a Eulerian fashion become important when a detailed study of currents in a particular region of interest is required on a long-term basis, either for operational applications or in academic interest. Such time-series measurements are particularly important for the design and installation of offshore structures and under-water pipelines. Current meters of many designs have also been used by biologists and oceanographers to determine the current velocities in marine waters. Present knowledge of currents in the world oceans has accumulated in part from time-series measurements made on different occasions through a variety of current meters deployed at different depths in different regions of the oceans. Long-term time-series measurements using an array of current meters have revealed several interesting phenomena.

In the past, the Eulerian method was mostly employed in situations where local time-series current measurements in the upper few meters of the ocean surface became necessary. At present, this method is used also for current measurements from much larger depths. Near-shore current

measurements using current meters mounted on solid bases and near-bottom measurements made with the aid of tripods or similar structures are representative of this method. Short-term measurements using a direct reading current meter (DRCM) hung from the side of country crafts, boats, or ships also come under this category.

Eulerian current measurements in the open ocean are usually accomplished using self-recording current meters attached to a taut-moored, surface, or subsurface buoy system and are capable of operating unattended for long periods of time. Deep-sea moorings are usually deployed with several current meters located at different depths. Although this method provides excellent time coverage, the current-versus-depth information is obviously limited to the number of current meters one can afford. Furthermore, in the design of oceanographic experiments using arrays of moored current meters, the question of their optimum spacing always arises. Because of the high cost, it is desirable to space the current meters as far apart as possible. On the other hand, the current meters must be close enough so that adjacent observations can be correlated. However, the question as to how close the current meters must be deployed in order that the observations can be correlated has not yet been fully answered.

For a given vertical distance, the coherence between the currents measured at a pair of current meters is considered the *correlation coefficient* between the two time series as a function of frequency. Webster (1972) observed that the

coherence estimates have the general property of being high at low frequency and dropping as frequency increases. He obtained an empirical relationship between the vertical separation of a pair of instruments and the frequency above which the coherence is less than a chosen critical value. However, the physical mechanism underlying this relationship has not been properly understood.

8.1. EULERIAN-STYLE MEASUREMENTS

This chapter addresses the Eulerian method of ocean current measurements. Eulerian current meters (sometimes referred to as *flow meters*) employ a wide range of sensors such as the Savonius rotor, unidirectional impellers, bidirectional propeller pairs, electromagnetic sensors, acoustic travel-time (ATT) difference sensors, and acoustic Doppler sensors. In some specialized situations, such as measurements of turbulence and very small flows, thermal and laser Doppler sensors are also used. Although all these sensors have varying degrees of merits and limitations, the choice of a particular type of sensor often depends on the type of study desired. A current meter intended for measurements in estuaries and inlets must be able to measure current flows as large as 300 cm/s or more. Because tidal variations in estuaries introduce variations in salinity and water temperature, and some locations have large sediment concentrations, the current meter must also be insensitive to these effects.

Eulerian current-measuring devices may be classified under the following categories:

1. Purely mechanical devices, whereby detection and recording of currents are controlled solely by mechanical devices
2. Current meters incorporating mechanical sensors, whereby detection of currents is achieved by mechanical devices, whereas acquisition and display/recording are controlled by electronic circuitries

3. Current meters whereby detection of currents is achieved by nonmechanical sensors and acquisition and display/recording are controlled by electronic circuitries

The present chapter primarily addresses mechanical sensors, which include Savonius rotor and vane, unidirectional impellers, and bidirectional propeller sensors. Some aspects of tow-tank measurements and calibration procedures are also discussed. Some of these current meters are direct reading types and others are recording types. In the former, current speed and direction as well as deployment depth are displayed on a deck unit in analog or digital display format, and the observations are noted by an observer on board (e.g., country crafts or research vessels) from where the current meters are deployed (Figure 8.1). Direct reading current meters are usually deployed for short-term *in situ* measurements of currents in coastal waters, estuaries, or ports where ship traffic and/or vigorous fishing activities render deployment of current meter moorings difficult. On the other hand, recording current meters on surface or subsurface moorings are usually deployed in offshore areas that are free from disturbances caused by fishing/navigational activities. Long-term time-series current measurements are desirable from shallow waters too but are not easy to obtain for various logistical reasons.

8.2. SAVONIUS ROTOR CURRENT METERS

Although the history of making current measurements in the ocean is long, the advent of user-friendly current meters is fairly recent. The Christian Michelsen Institute in Bergen, Norway, contributed immensely to the initiation and development of various types of current meters. At this institute, Ivar Aanderaa was the main contributor in this field. Aanderaa designed the classic current meter in the late 1950s (Aanderaa, 1964) using a Savonius-like rotor (Savonius, 1931) and a magnetic compass as the speed- and

FIGURE 8.1 (left) Deployment of a direct-reading-type Savonius rotor current meter from a country craft; (right) current speed and direction and deployment depth displayed on a deck unit being noted by an observer on board the country craft. (Source: Courtesy of CSIR-National Institute of Oceanography, India.)



direction-sensing elements, respectively. This current meter, universally known as the Aanderaa Current Meter, has thereafter been the “workhorse” of oceanographic current measurements and is traditionally used for deep-ocean, shelf, and estuary researches. The Savonius rotor’s insensitivity to variations in the surrounding environmental conditions is its noteworthy feature, making it suitable for current flow measurements in estuaries and inlets. The first-generation Aanderaa current meter senses scalar speed above a threshold of 2 cm/s and relies on a large vertical fin to orient the entire instrument in the direction of current flow. The current meter remains vertical in steady conditions at mooring wire angles of up to 27°; from the vertical. Despite the advent of more sophisticated current meters in the 1980s, rotor current meters continued to be improved by M/s. Aanderaa Instruments and are being used by several oceanographers from across the world.

Measurement of currents using a mechanical sensor such as a rotor is based on the mechanism of physical rotation of the rotor in response to the drag force it experiences from the moving water in a flow field. For steady flows, the average rotational frequency of the rotor is closely related to the speed of the fluid impinging on it. The first-generation Aanderaa Savonius rotor (see Figure 8.2) permitted it to rotate in the same sense, irrespective of the direction of current flow. A small magnet embedded at the bottom end of the rotor stud permits detection of its revolution by magnetically coupling it to a sensing device such as a reed relay, magneto diode, or inductor that is rigidly mounted in the watertight housing immediately beneath the rotor. Speed is sampled by summing the revolutions of the rotor over a defined sampling interval (the sum of pulses



FIGURE 8.3 Aanderaa north-seeking magnetic compass. (Source: Aanderaa Instruments Model 4 Recording Current Meter Manual.)

corresponding to rotor revolutions over ~32 seconds in the case of the Aanderaa rotor shown in Figure 8.2 provides an approximate value of current speed in cm/s). The speed of the water current is precisely calculated from the steady-state calibration equation for the sensor. The measured speed is, therefore, an integrated or averaged speed over the measurement interval.

A method popularly used for determination of the direction of water current flow relative to Earth’s magnetic north is to rigidly couple a magnetic compass (see Figure 8.3), which is mounted within the current meter (CM) housing, to a large tailfin that is rigidly fixed to the CM housing (see Figure 8.4). With this technique, the



FIGURE 8.2 Initial design of the Aanderaa Savonius rotor, capable of rotating in the same sense irrespective of the direction of current flow. A small magnet embedded inside the bottom end of the rotor stud permits detection of its revolution by magnetically coupling it to a sensing device rigidly mounted in the watertight housing immediately beneath the rotor. (Source: Aanderaa Instruments Model 4 Recording Current Meter Manual.)

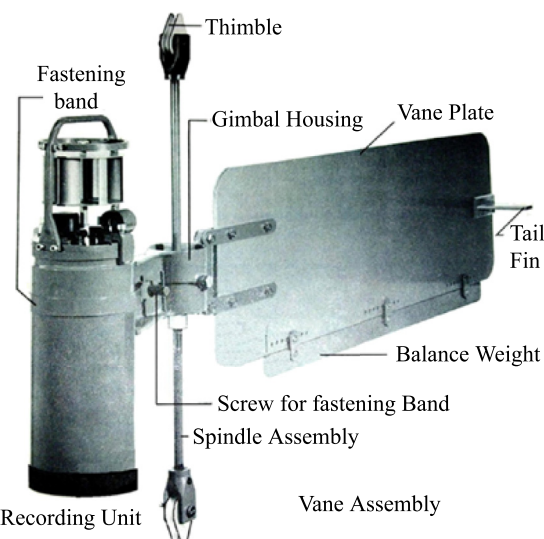


FIGURE 8.4 Aanderaa Savonius rotor current meter housing rigidly coupled to a large tailfin for automatically orienting the current meter in the direction of current flow. (Source: Aanderaa Instruments Model 4 Recording Current Meter Manual.)

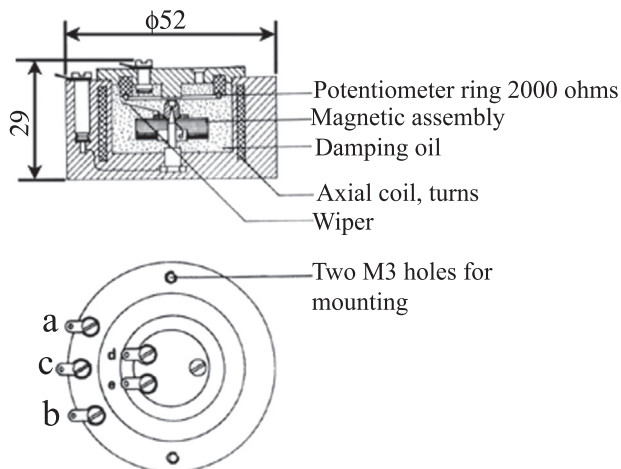


FIGURE 8.5 Constructional details of Aanderaa magnetic compass. (Source: Aanderaa Instruments Model 4 Recording Current Meter Manual.)

whole CM is constrained to rotate in tune with the changing current direction. The magnetic compass gives the orientation of the fin and, therefore, the direction of current flow relative to Earth's magnetic north, obeying the universal convention of water current direction, namely "current toward." (Note that the universal convention of wind direction is "wind from.") The construction details of the magnetic compass are shown in Figure 8.5.

M/s. Aanderaa Instruments has pioneered in rotor current-meter technology, and several of their devices have been deployed in the world oceans. The current meter (see Figure 8.6) is deployed on a mooring line. Aanderaa rotor current meters are self-contained instruments that can be moored in the sea and can record ocean current, electrical conductivity, and temperature of the water, together with deployment depth (CTD). Construction details of the vane assembly and the mechanism for supporting the Aanderaa CM housing are shown in Figure 8.7. The combination of recording unit and vane assembly is equipped with a rod that can be shackled into the mooring line (see Figure 8.8). This arrangement permits the instrument to swing freely and align with the current. The recording unit contains all sensors, the measuring system, battery, and a detachable, reusable data storage tape unit (see Figure 8.9). In later modifications, the tape was replaced by a solid-state data storage device.

In operation, a built-in clock triggers the instrument at preset intervals and a total of six channels are sampled in sequence. The first channel is a fixed reference reading for control purposes and data identification. Channels 2, 3, and 4 represent measurement of temperature, conductivity, and depth, respectively. Channels 5 and 6 represent the vector-averaged water current speed and direction since the previous triggering of the instrument. The data are sequentially fed to a data storage unit (DSU). Simultaneously, as the reading takes place, the output pulse keys on and off an acoustic carrier emitted by an acoustic transducer. This

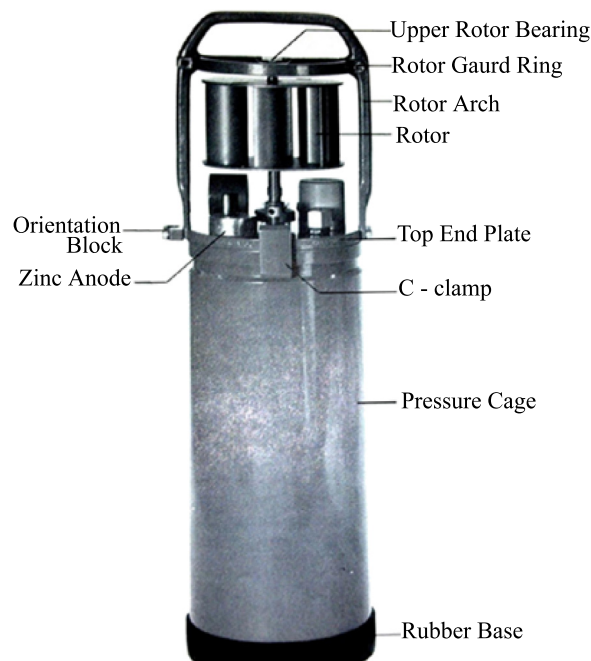


FIGURE 8.6 Constructional details of the Aanderaa Savonius rotor current meter. (Source: Aanderaa Instruments Model 4 Recording Current Meter Manual.)

allows monitoring of the performance of the moored instrument from the surface by a hydrophone and can be used for real-time telemetry of data. The recording interval of the instrument is set by an interval selector switch. When a 10-minute interval is used, the operating period of the instrument will be two months. Aanderaa current meters are available in different depth ranges.

Until about 1987 a very simple sampling scheme was used in the Aanderaa current meter: The number of rotor revolutions during a predetermined sampling interval was recorded on magnetic tape, together with a single spot measurement of the meter orientation, derived from the mechanically clamped compass. Analog-to-digital conversion of the six available data channels was accomplished by an electromechanical encoder controlled by a crystal clock. The same encoder was used to drive the magnetic tape transport system and to actuate the parameter-selecting switch. In subsequent modifications M/s. Aanderaa Instruments incorporated a vector-averaging sampling scheme and solid-state memory. Samples are taken every 12 seconds and are decomposed into east and north components. Successive east components and successive north components are added separately, and the vector-averaged speed and direction are computed at the end of the measurement interval and then recorded in the data storage media. The capacity of the system is 10,900 sampling cycles, which, for example, provides 75 days of operation at 10-minute sampling intervals.

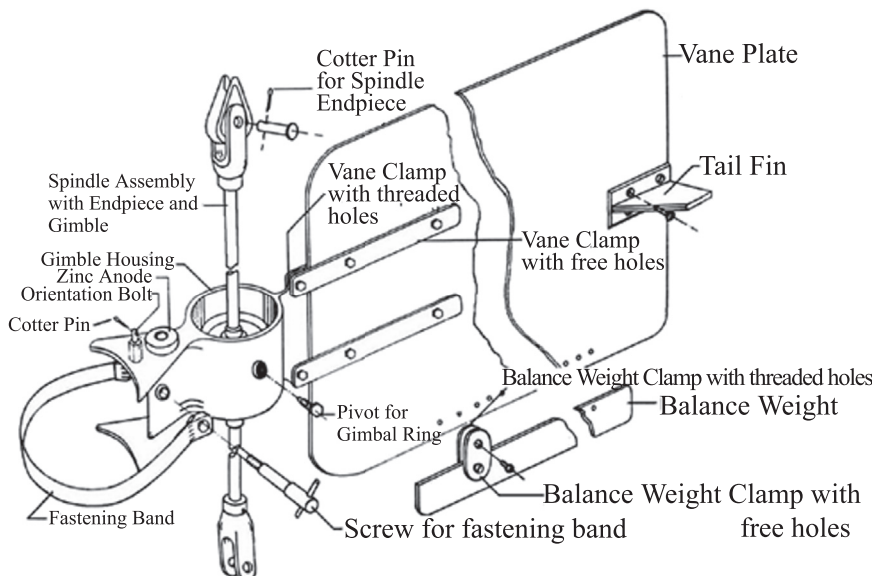


FIGURE 8.7 Constructional details of the vane assembly and the mechanism for supporting the Aanderaa current meter housing. (Source: *Aanderaa Instruments Model 4 Recording Current Meter Manual*.)

Over the years, the first-generation Aanderaa Savonius rotor-type current meter established an enviable reputation for durability and reliability. Reasonable price was another attraction. There is widespread experience of its use in the major oceanographic institutions and in industry. Because the first-generation Aanderaa CMs were used by several oceanographers and environmentalists over a long time, these were also the ones that were evaluated the most. Based on these studies it has been observed that the usefulness and accuracy of a CM incorporating a Savonius rotor for measurement of small currents is related to the sea state, the degree of unsteadiness of the current flow, and the mooring style. Paquette (1962) pointed out that a rotor-type CM exhibits over-registration when the mean flow is weak. Pollard (1973) reported that error currents as large as 20 cm/s could be recorded by surface-moored rotor CMs in severe wave conditions. Karweit (1974) observed systematic errors in Savonius rotor current measurements in unsteady currents as inferred from steady-state calibrations and small overestimates of low-frequency current measurements by a vector-averaging rotor CM in the presence of intense high-frequency oscillatory currents.

It has also been observed that the rotor tends to respond differently at different frequencies of the oscillatory current. Field experiments conducted by Halpern and Pillsbury (1976) revealed that as a result of mooring motion, the rotor is “pumped round” and often senses an excess speed, an effect popularly known as *rotor pumping* or *over-speeding*. Saunders (1980) noted that a Savonius rotor is also sensitive to vortices shed by the CM’s body. Comparison of rotor CMs on surface moorings showed that rotor pumping by mooring motion is a major limitation. If

rotor pumping adds a constant speed to the current measurement record, the observed energy will be elevated by an approximately constant proportion across the entire spectrum (Pearson et al., 1981). In high sea-state conditions, there is a high probability of contamination of current measurement records by rotor pumping. The influence of

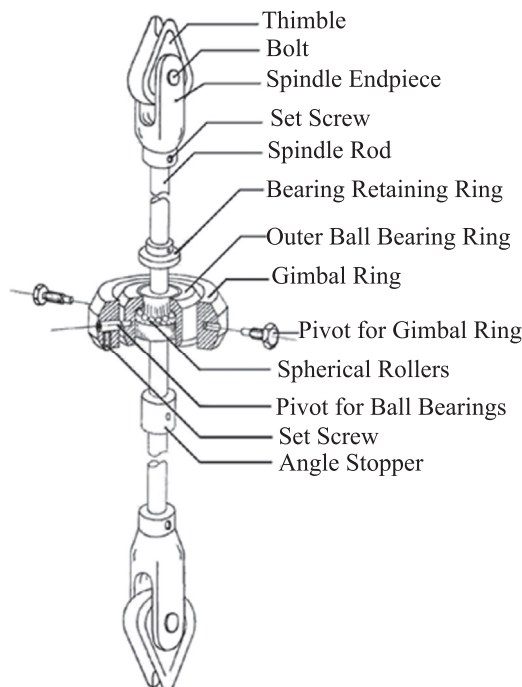


FIGURE 8.8 Constructional details of the rod that is shackled into the mooring line of the Aanderaa current meter. (Source: *Aanderaa Instruments Model 4 Recording Current Meter Manual*.)

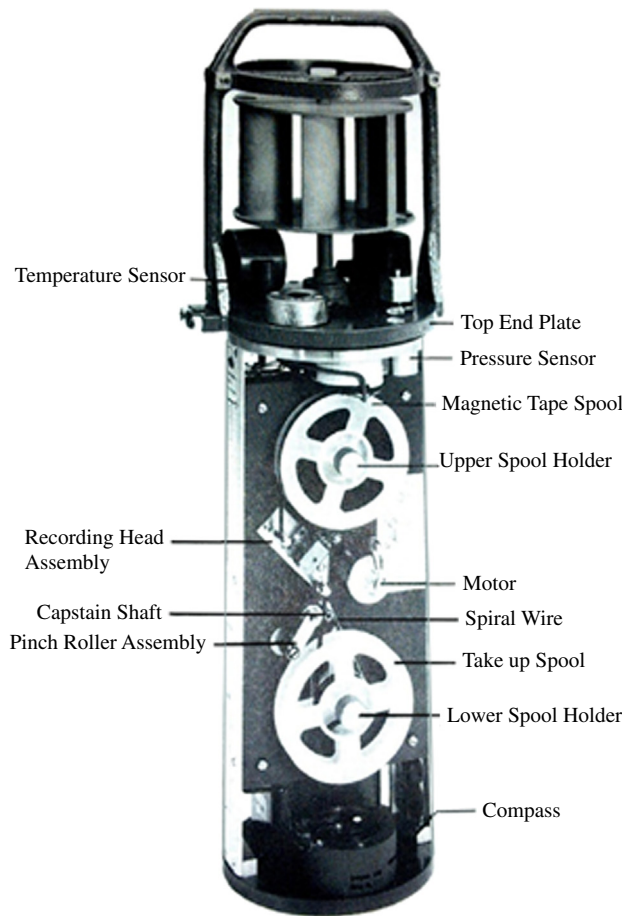


FIGURE 8.9 Aanderaa Savonius rotor-style recording current meter containing all sensors, the measuring system, battery, and a detachable, reusable data storage tape unit. (Source: Aanderaa Instruments Model 4 Recording Current Meter Manual.)

wave motion decreases exponentially with depth; therefore, the depth of the subsurface float is a critical factor in using Savonius rotor-type CMs.

Field experiments conducted by Halpern and Pillsbury (1976), Halpern et al. (1981), and Johnson and Royer (1986) revealed that the surface-moored rotor-type CM exhibits over-registration when the mean current is small and the oscillatory currents are large. Schott et al. (1985) found that the error can be reduced but cannot be fully eliminated by adopting improved mooring techniques.

It was found that even the fin can introduce some errors in the measurements. The large-fin system suffers from long response time and is therefore unsuitable for accurate current measurements under large turbulence. Kenney (1977) analyzed the dynamics of such a direction-orienting fin and noted that the use of a long fin to orient a CM into the “mean” current requires caution. For example, when a Savonius rotor CM is deployed in a turbulent flow regime, the measured “mean” current could be grossly overestimated, depending on the intensity and spectrum of the

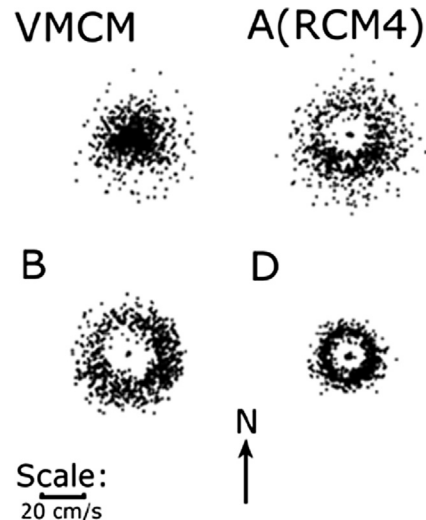


FIGURE 8.10 Presence of “holes” in the Savonius rotor current meter’s current velocity distribution at low speeds (less than 50 cm/s). (Source: Sherwin, 1988.)

lateral component of turbulence. The orbital velocity of the oscillations at the sea surface due to waves, especially due to swells, penetrates to great depths following an exponential law related to the angular velocity and amplitude of the wave at the sea surface. This indicates that the mean current at depths below a persistent wave- or swell-ritten sea is superimposed by oscillatory motions. If the CM deployed in such an environment employs a large direction-orienting fin rigidly coupled to the CM’s body, it is likely that the CM may undergo some degree of angular motion. Such motions result in the rotor’s nonlinear response because the axis of the CM swings through an arc (Sherwin, 1988). In a nutshell, it was observed that although well suited to measurements in steady flow regimes, the first-generation Aanderaa CMs are considered unsuitable for applications in or near the surface wave zone or indeed wherever appreciable instrument motion is likely to occur (Saunders, 1976; SCOR WG 21, 1974).

Field intercomparison studies conducted by Johnson and Royer (1986) indicated that speed measurements obtained from rotor CMs are influenced by the effect of rotor pumping. This effect is manifested by the presence of “holes” (see Figure 8.10) in the current-velocity distribution at low speeds (less than 50 cm/s). The observed hole is indicative of the absence of low speeds at rough-sea conditions. With reduced wave activity, the size of these “holes” is also reduced and the holes finally became absent in calm-sea conditions. Sherwin (1988) observed a mean-speed overestimation of 66 percent by the Savonius rotor-type CM when current-flow speeds were less than 10 cm/s and waves and swells were large. Analytical treatment of moored CM motion (Griffin, 1988) indicated that it is necessary to minimize the phase difference between the

current-flow velocity and the CM's velocity to minimize the relative oscillatory current detected by the rotor.

Analysis of Savonius rotor performance in varying current-flow conditions, field intercomparison studies, and analytical treatment of mooring motion in oscillatory flows as just mentioned indicate that amplification of rotor CM speed measurements will be greatest when the mean currents are small and high-frequency oscillatory flows are of larger amplitudes. In summary, a surface-moored Savonius rotor CM is unable to record small horizontal currents at high sea states when other types of sensors record small currents under similar sea states.

In an attempt to unravel the mysteries that shroud the motion of a Savonius rotor in an unsteady current, various investigators have performed numerous laboratory experiments. A series of independent experiments conducted by Fofonoff and Ercan (1967) and Saunders (1980) in wave tanks provided contradictory results as to the response of the rotor in accelerating and decelerating flows.

One line of thought attributed current-speed over-registration by Savonius rotors during small current flows to the two end plates, which support the curved blades of the rotor. The argument often put forward is that, in this configuration, the rotor is likely to "trap" a certain amount of water during its rotation and, therefore, increases its inertia. In an attempt to improve the rotor CM's performance, a new version of the Savonius rotor was introduced by M/s. Aanderaa Instruments. This new version is devoid of the end plates, and the curved blades are replaced by a set of flat-bladed paddlewheels that are distributed in diametrically opposite directions (see Figure 8.11). This arrangement (incorporated in Aanderaa RCM 7 current

meter) necessitates covering half the portion of the rotor (in the direction of current flow) to allow its unidirectional rotation in the presence of current flow (see Figure 8.12). Various stages of deployment of an Aanderaa RCM 7 current meter are shown in Figure 8.13.

Replacement of the Savonius rotor by a "flat-bladed" paddlewheel design and modifications to the vane was expected to improve the performance of the CM in the near-surface region, though prior to the introduction of vector averaging the fundamental limitations in directional measurement remained (Woodward, 1985). As yet relatively little information is available on the effectiveness of the more recent changes, though Loder and Hamilton (1990) have reported on some effects of high-frequency mooring vibration.

Obviously, the half-cylindrical cover now used in the Aanderaa RCM, having a possible drawback of shedding of eddies from its edges, could have been avoided if the flat-bladed paddlewheels were replaced by curved-bladed paddlewheels having no end plates. When the author of this book put forward this suggestion to Ivar Aanderaa in March 1995, he went from the visitors' room and came back with a rotor that had curve-bladed paddlewheels devoid of end plates (see Figure 8.14), which resembled the one that I suggested. He told me with a smile, "My wish was to use this rotor; but somehow it did not materialize." Because the two ends are "open" in either of these configurations, the

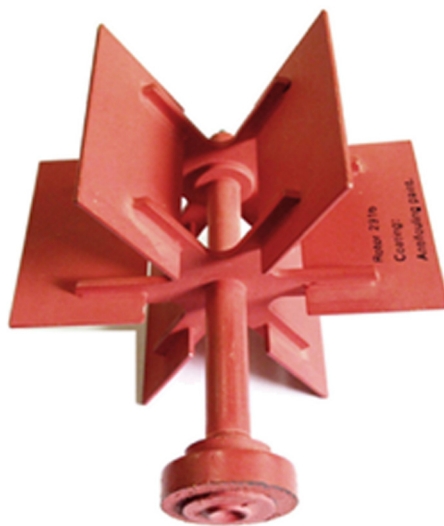


FIGURE 8.11 M/s. Aanderaa Instruments' modified version of the Savonius rotor. A set of "flat-bladed" paddlewheels without end plates is uniformly distributed in diametrically opposite directions. (Source: Aanderaa Instruments Current Meter Manual.)

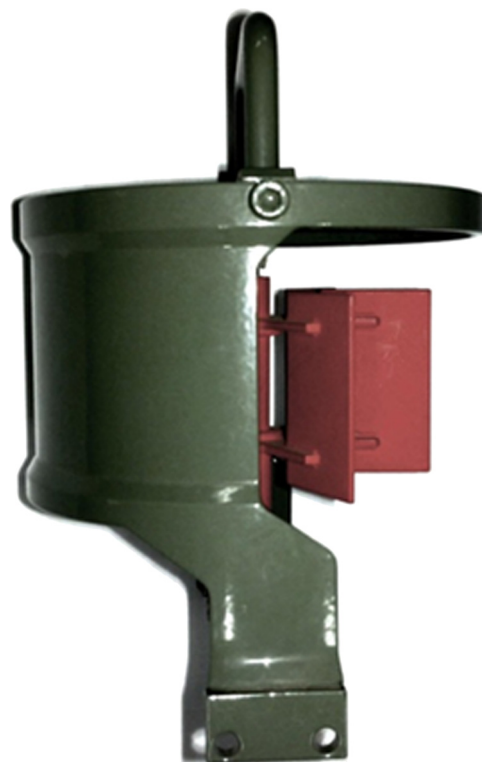


FIGURE 8.12 Half-cylindrical cover of the "paddlewheels" rotor to allow unidirectional rotation of the rotor in presence of current flow. (Source: Aanderaa Website: www.aanderaa.com.)

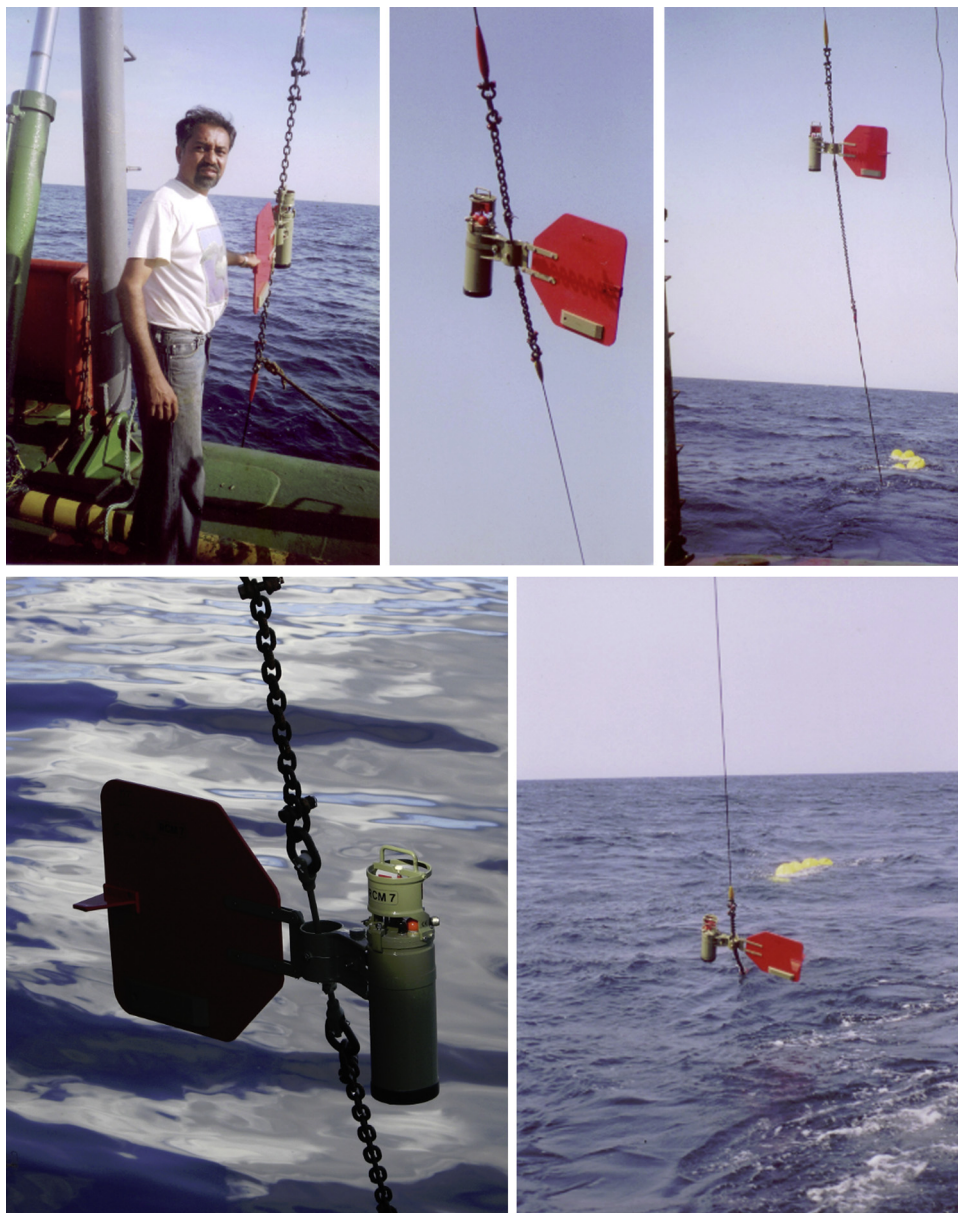


FIGURE 8.13 Various stages of deployment of an Aanderaa RCM 7 current meter. (Source: Courtesy of Vijayan Fernando, CSIR-National Institute of Oceanography, Goa, India.)

problem of increase in inertia due to water trapping is expected to be eliminated. To this author's knowledge, no performance evaluation of the modified rotor vis-à-vis the old version of the Savonius rotor in terms of rotor pumping effect had been reported. The fact that a cup anemometer with no end plates also exhibits overspeed registration in a turbulent wind field (Busch et al., 1976) is probably an indication that removal of end plates of the Savonius rotor may not be a remedy against overspeed registration by the Savonius rotor. In any case, there appears to be no experimental evidence as to the real cause of overspeed registration by Savonius rotors, and therefore it may be premature to attribute “overspeed registration” to “rotor overspeeding.”

Looking at the problem of overspeed registration (during weak currents) by surface-moored Savonius rotor CMs from a purely instrumentation point of view, Joseph (1991) proposed that one of the reasons for this problem could be slow bidirectional rotation of the rotor, instead of the expected unidirectional rotation, in a weak or no-flow situation. When the mean horizontal current is weak and the Savonius rotor CM moves up and down under the influence of mooring-line motion, it is quite possible that the rotor might tend to make slow bidirectional motions about its axis. This is because the horizontal drag force, which is responsible for the unidirectional rotation of the rotor, is negligible at very weak currents.

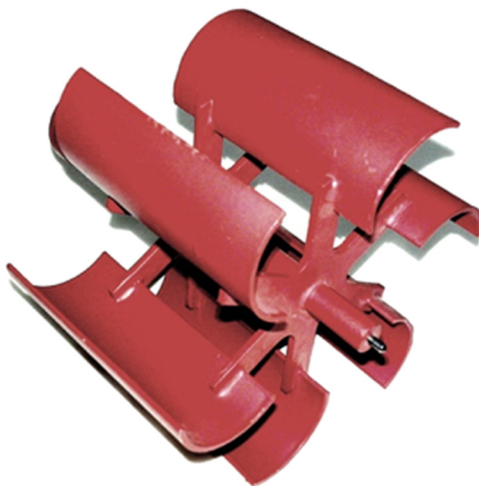


FIGURE 8.14 Rotor with curved-bladed paddlewheels devoid of end plates, which would have avoided the use of the half-cylindrical cover. (Source: Courtesy of the late Ivar Aanderaa, Aanderaa Instruments, Norway.)

If the rotor executes bidirectional motions, the reed relay (which is magnetically coupled to the rotor and used for detecting the current speed) can close and open whenever it happens to be within the magnetic field of the embedded magnet at the end portion of the rotor's stud. The technique devised by Joseph (1991) to detect and tag the anticipated bidirectional rotation of the rotor consists of three reed relays, each of which is rigidly mounted within the waterproof housing of the CM at an angular separation of 120° and is located within the magnetic field of the rotor. A rotor-following magnet, which is free to rotate about the principal axis of a ball bearing and to freely sweep over the three relays, is so positioned that only one pole of the magnet can effect a closure of the relay. Thus, one full revolution of the rotor in the same sense will result in serial closures of all the three relays, thereby generating three electrical pulses during one full revolution of the rotor.

The electronic circuit incorporating the three relays generates a frequency-shift-keyed (FSK) signal (i.e., closure of each relay is represented by a unique pulse-stream frequency). If the rotor rotates unidirectionally in the correct sense (i.e., as expected in a steady current flow), the circuit registers the correct counts during the current-speed measurement interval. If there is no flow, no count is registered. If, however, the rotor undergoes bidirectional motions about its axis (i.e., the rotor's motion is not due to a steady current flow), the flow-unrelated rotations of the rotor during the current-speed measurement interval are also registered. Thus, the device enables counting the rotor-generated electrical pulses in a form that permits detection of error counts produced by the bidirectional motions of the rotor. In this way, the device prevents attribution of an erroneous higher value to current speed when the mean current is absent or it is actually very weak.

8.3. SAVONIUS ROTOR AND MINIATURE VANE VECTOR-AVERAGING CURRENT METERS

Some of the problems associated with the first generation of the Aanderaa Savonius rotor CM incorporating a large direction-orienting vane arose primarily from the scalar averaging of speed and the inadequate sampling of direction. The CMs that came to be known as vector-averaging current meters, or VACMs (McCullough, 1975), the first of the VACMs, offered substantially improved performance over the first generation of the Aanderaa CMs in nonsteady flows. When this was realized, the vector-averaging procedure was incorporated in the second-generation Aanderaa rotor CMs.

In the VACM the measurement is made of polar components using a Savonius rotor, the rotation of which is sensed eight times per revolution, and a miniature vane (9×17 cm) is used to indicate flow direction (see Figure 8.15). The direction orientation of the vane relative to the "zero" of the magnetic compass (which is rigidly mounted inside the in-water housing of the current meter) is measured to determine the direction of water-current flow in the conventional style. At each rotor count, the sine and cosine of the flow direction relative to magnetic north are computed from measurements of compass and vane-follower outputs and are accumulated in east-west and north-south registers over the sampling interval so as to provide a vector-averaged mean. Though representing a considerable improvement over CMs employing simple sampling schemes, the VACM falls short of ideal

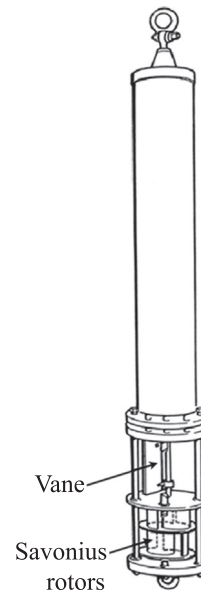


FIGURE 8.15 Vector-averaging current meter (VACM) with a miniature fin capable of free motion about the axis of the instrument housing. (Source: Beardsley, R.C. 1986.)

performance in oscillatory flow, due partly to inadequacies inherent in the rotor and vane dynamic response characteristics (Fofonoff and Ercan, 1967), and partly to rotor pumping. This last effect is the name given to the rectification of eddies shed by supporting structures and the instrument case, particularly when the instrument is subjected to strong vertical motions. Horizontal oscillatory flows can cause either underspeeding or overspeeding, depending on the characteristics of the flow and the amplitude of the fluctuations relative to the mean. The response of the Savonius rotor to a change in flow conditions may be characterized in terms of the filament length of the fluid that must pass through the rotor before adjustment to the new fluid speed is complete. The time constant is thus dependent on fluid speed, the rotor responding more closely to an increase than to a reduction in fluid speed. An estimate of the likely effects of rotor time constants on accuracy has been provided by Saunders (1980), who measured response lengths in both accelerating and decelerating flows. Application of these values in a simple

rotor model of the form $\frac{dR}{dt} = \frac{(S - R)}{t}$ subjected to simple harmonic periodic forcing (where R is the rotor speed converted to apparent flow speed, S is the true speed, and t is the rotor time constant) generated maximum fractional errors of ~10 percent when oscillatory and mean current values were comparable in magnitude.

A similar form of model was also used to examine the vane and the vane-follower responses (Saunders, 1976). In this instance, $\frac{d\theta}{dt} = \frac{(\theta_i - \theta)}{t}$, where θ_i , θ are, respectively, the instantaneous current and vane directions, and $t \geq 1.5$ sec is the combined vane and vane-follower time constant. When applied to some representative near-surface current data, an overreading of currents of order 10 percent was predicted by the model. For a discussion of the importance of vane characteristics, refer to Kenney (1977). More recent work by Patch et al. (1990, 1992) considers the dynamic response characteristics of the VACM compass and vane follower.

In the case of a direct reading current meter (DRCM) incorporating a fixed and large direction-orienting vane, the motions of its cable and the current meter's in-water housing may cause additional errors in the measurement of the mean current velocity. These problems can be circumvented by incorporation of a miniature vane that is capable of free movement with respect to the axis of the instrument housing. However, unlike the fixed-vane configuration, a constant heading of the CM's in-water housing relative to the direction of current flow cannot be maintained in a free-vane configuration. Consequently, variation of the horizontal angles between the current-flow direction and the supporting rods of the rotor causes errors in the flow-speed measurements (Pite, 1986; Joseph and Desa, 1994).

8.4. PROPELLER ROTOR CURRENT METER (PLESSEY CURRENT METER)

While the Savonius rotor CMs were already in wide use, searches were in progress for the design of a different style of CM using a different sensing device. Hedges (1967) reported the design and development of a propeller-type rotor current meter. He carried out the work at the Christian Michelsen Institute in Bergen, Norway, under the auspices of the NATO Subcommittee for Oceanographic Research, with cooperation and help from Odd Dahl and Ivar Aanderaa from the Institute in Bergen. (Aanderaa later left Christian Michelsen Institute and started a private company, Aanderaa Instruments.) Subsequent to completion of the basic design and development in Bergen, particularly the novel electromechanical analog-to-digital converter that also drives the magnetic tape transport system and actuates the parameter selecting switch, the basic instrument was then further engineered at the Marine Systems Division of the Plessey Company Ltd. to make use of a propeller-type rotor, in place of the Savonius type rotor fitted to all previous prototypes, to measure current flows.

The Plessey Recording Current Meter (see Figure 8.16) was designed primarily to measure and record data on the speed and direction of water flow. The method by which the instrument measures the current flow is by obtaining the total rotor revolutions over a known period of time. The total revolutions are divided by the time to give an average speed in revolutions per second, which can be directly related to the flow in feet per second from a calibration graph. There is no means of knowing whether the total revolutions measured occurred at the average rate or at some other varying rate. To avoid error due to the assumption of an average rate, the rotor calibration needs to be linear.

The main factors considered in the propeller design were to achieve linearity, low-speed response, good mechanical strength, reliability, and ease of servicing. Linearity is obtained by designing the propeller to give



FIGURE 8.16 Plessey propeller-type current meter. (Source: www.aagm.co.uk/thecollections/objects/object/Plessey-Current-Meter-And-Fin-Mo21—Serial-Number-267?.)

a minimum of interference between blades and by ensuring that the blades never operate in a semi-stalled condition. Consideration of a suitably sized propeller makes this a three-bladed design of a length to permit the trailing edge of a blade to be in line with the leading edge of the following blade (see Figure 8.17). By the selection of a suitable length, this results in a convenient nominal pitch of 1 foot. For low-speed response with consistent performance over a long immersed period, the bearing design is based on a watch-type escapement pivot. The assembly is also spring-loaded to give adequate mechanical protection. The pivot material is stainless steel and the bearing bush is loaded nylon. To reduce weight on the bearing, the material chosen for the propeller itself is plastic. Mechanical strength and reliability are achieved by the sprung design of the bearing bush, which permits the whole assembly to move sideways until the hub is supported by the main frame (see Figure 8.17).

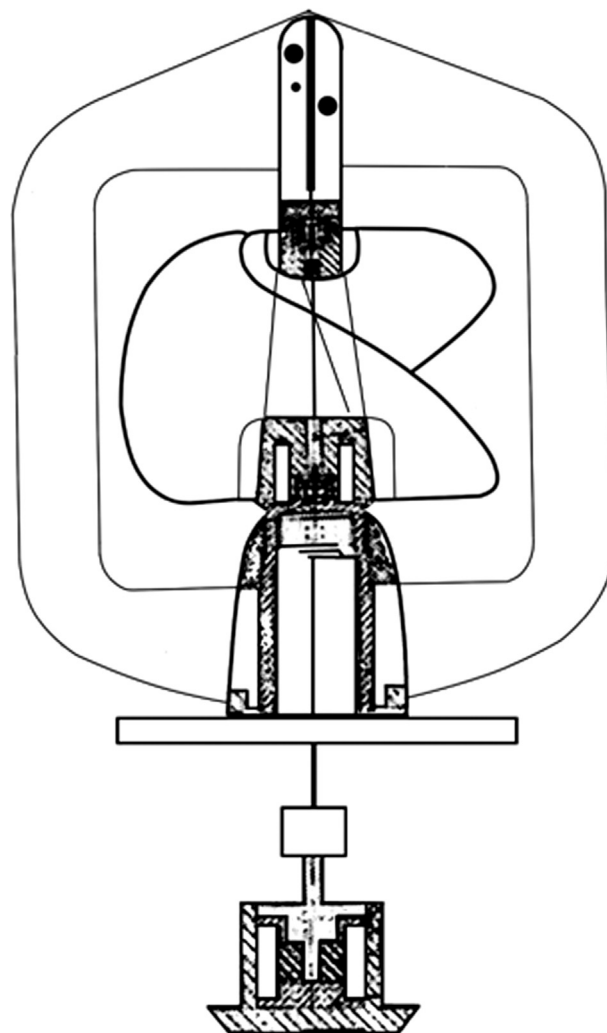


FIGURE 8.17 Details of mounting of Plessey propeller. (Source: Hodges, 1967.)

Very heavy side shock loads are supported in this manner and do not damage the pivot. This feature also provides a self-aligning action, which means that performance is maintained even if the outer frame is partially distorted. The hub is also shrouded at both the front and the rear by suitable skirt extensions, which are designed to prevent fouling from weed and growth. The whole propeller is painted with antifoulant. For ease of servicing, the front bearing assembly can slide forward. This releases the propeller, which can be extracted through the side supports and gives immediate access to the bearing assembly. Based on performance data obtained from the Wallingford Hydraulics Research Station, the minimum starting speed is 2.03 cm/s. The stopping speed is 1.98 cm/s. It was found that good linearity is maintained from 4 to 250 cm/s. Coupling of the propeller to the instrument proper is made by magnets inserted within the propeller hub immediately on each side of the bearing housing. This magnet drive operates a concentric gearbox housed within the support pillar, which also carries the propeller bearings and bearing frame. The final driven potentiometer is built as an integral part of the gearbox, and the overall loading on the propeller has been kept to a minimum by this method.

A major change introduced in the Plessey meter is the method of suspension from the mooring cable. It can be appreciated that to make good use of the propeller-type rotor for measuring current flows, it is essential that the propeller face correctly into the direction of the water flow. It is little gain to have a propeller sensitive to low velocities if it is not also able to swing into the flow direction under the same low-flow velocity conditions. One method adopted to give low-velocity alignment response is to have less frontal area, which means that less fin area is needed. An additional scheme is the use of an offline suspension system. In the use of this system, the instrument only is suspended below the pivot. This reduces the overall hung weight, and the load on the pivot is reduced.

To suit practical use of the meter, all the instrumentation and power supplies are contained in a cylindrical pressure-sealed tube that is 5 inches in diameter and 15 inches long. This tube is suspended in the water and has attached to it small directional fins and a propeller-type rotor that drives through a magnetic coupling to the internal instrumentation so that the basic cylinder is completely sealed and self-contained. Standard domestic magnetic tape is used for recording and storing the information from the speed and direction sensors. The information is related to variations in resistance ratios and is converted to 10-bit binary numbers and recorded onto magnetic tape in the form of long and short DC pulses. The binary number code is obtained from an electromechanical analog-to-digital converter, which is generally referred to as the *encoder*.

The current speed is obtained from a change in a resistance ratio over a period of time of a potentiometer, driven

by the rotor via a magnetic coupling and a reduction gear as mentioned earlier, with the rotor being turned by the water current. Current direction is obtained from a magnetic compass that is made to include a potentiometer resistance element; at the start of a direction measurement, a floating contact clamps to the potentiometer to provide the required resistance ratio, which is proportional to the angle with reference to the Earth's magnetic north.

A further feature of the design is the inclusion of a fixed resistance ratio within the instrument, the repeated measurement of which is used to identify the individual instrument. This is referred to as the *reference*. The whole system is powered by batteries and controlled by a separate battery-driven clock mechanism that initiates the measuring cycle at preset time intervals.

For telemetry and direct reading of the data, the pulses (which represent the data) fed to the recording head of the tape recorder are propagated through the water as an acoustic signal via a spherical transducer mounted on the top plate of the instrument. These pulses can be picked up and monitored on a suitable hydrophone receiver at ranges up to 500 meters.

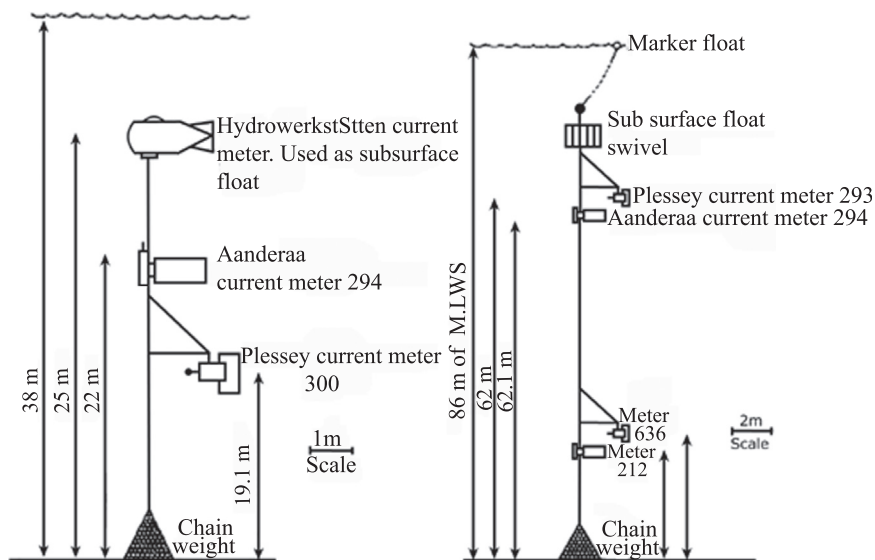
The receiving hydrophone is used on board a surface vessel and can accept the pulses and convert these into an audible note that can be listened to and recorded or fed into a pen recorder or special printout unit, which will show the pulses as short and long dashes. The long pulses represent binary 0 and the short pulses binary 1; knowing this, the binary number can be converted to its equivalent decimal number. Thus, a direct-reading facility is made available by this means.

Ramster and Howarth (1975) reported a detailed comparison of the data recorded by Plessey MO21 and Aanderaa Model 4 recording current meters (the ones that incorporated the first-generation Savonius rotor shown in

Figure 8.2) moored in two shelf-sea locations in the North Sea and the Irish Sea, each with strong tidal currents. Schematic diagrams of the moorings of these two current meters are shown in Figure 8.18. Obtained comparison measurements are shown in Figure 8.19. The instruments measured integrated counts from the speed sensor and discrete directions from the direction sensor every 10 minutes. In general, there were no very strong winds during the measurements, so that a comparison of performance in rough seas is not possible. It is apparent that in the calm-sea conditions of the present measurements, there is very good agreement between the data recorded by the two types of current meters every sample interval. Calculation of "stream prediction" residuals (residual current is the measured current minus the predicted tidal current) is expected to highlight the differences in the sets of data not readily apparent in the straight computation of tidal constituent characteristics and shows up the full implications of apparently small and unimportant differences. Based on the use of this scheme, it was found that there is very good agreement between the residuals calculated from the data recorded by the two types of current meters. Fortunately, there was a small window during which relatively strong wind blew during the measurement, and this provided a fortuitous opportunity to examine the residuals from the near-surface meters (see Figure 8.20). In general, the hourly estimates of residual speed for the near-surface meters agree to within 4 cm/s and for the near-bottom meters to within 2 cm/s (see Figure 8.21). The fact that the residuals agree so well in the presence of strong tidal currents is encouraging.

As indicated earlier, a known drawback of the Savonius rotor is that its omnidirectional properties do not allow it to record currents faithfully in the presence of waves

FIGURE 8.18 Schematic diagram of the moorings of the Plessey MO21 and Aanderaa Model 4 recording current meters moored in two shelf-sea locations. (Source: Ramster and Howarth, 1975.)



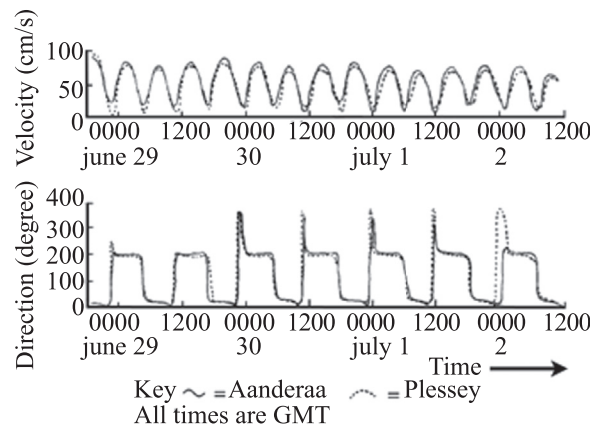


FIGURE 8.19 Time-series current speed and direction measurements obtained from Plessey MO21 and Aanderaa Model 4 recording current meters moored in two shelf-sea locations. (Source: Ramster and Howarth, 1975.)

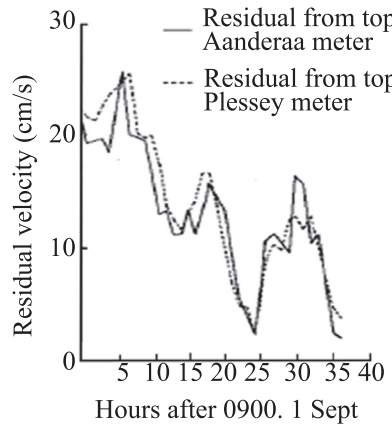


FIGURE 8.20 The magnitude of a surge recorded by the near-surface moored Plessey MO21 and Aanderaa Model 4 recording current meters. (Source: Ramster and Howarth, 1975.)

(Hansen, 1964). This is because the orbital velocity of water particles due to wave action will always add to the speed seen by the rotor, whereas an impeller's speed of rotation will only correspond to the current flowing axially to it and will reverse if the flow reverses. If the direction of the waves and the tidal stream is the same and if the speed of the tidal stream is in excess of the orbital velocity due to waves, then both the rotor and the impeller will record the same current speed. The rotor, however, will record higher speeds than the impeller for tidal stream speeds that are lower than the orbital velocity. In a moored system where the subsurface float is influenced by the surface waves, the surface-wave action on the subsurface buoy is being taken up by the mooring wire, leading to the movement of even the bottom instruments to and fro in the water. The omnidirectional sensitivity of the rotor of the Aanderaa meter would then lead to velocities being recorded that are higher than those measured by the Plessey meter. A scatter plot of

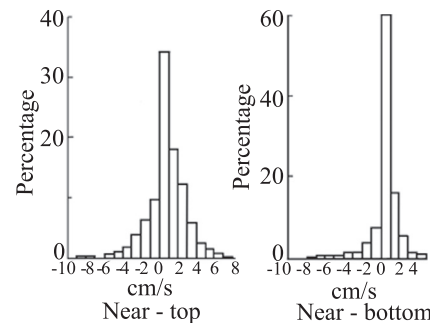


FIGURE 8.21 Percentage-frequency diagrams of the differences (cm/s) between the hourly estimates of residual drift as calculated from the two sets of intercalibration data from the near-surface moored Plessey MO21 and Aanderaa Model 4 recording current meters. (Source: Ramster and Howarth, 1975.)

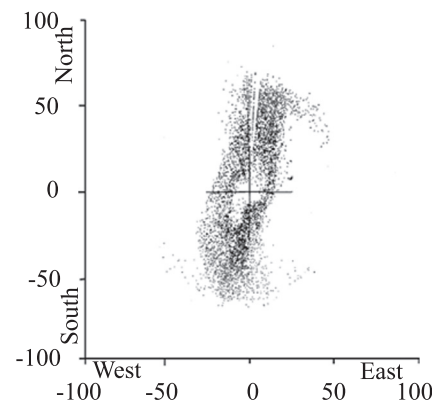


FIGURE 8.22 A scatter plot of the velocity components calculated from the near-bottom Aanderaa data. (Source: Ramster and Howarth, 1975.)

the velocity components calculated from the near-bottom Aanderaa data is shown in Figure 8.22. It may be recalled that appearance of “holes” in the scatter plot of Savonius rotor current meter data was indicated in Section 8.2.

8.5. BIAXIAL DUAL ORTHOGONAL PROPELLER VECTOR-MEASURING CURRENT METERS

The biaxial dual orthogonal propeller current meter measures averaged orthogonal components of the flow with two pairs of orthogonally mounted dual propellers (i.e., two propellers fixed on one axle) with accurate cosine-response characteristics. The term *cosine response* refers to the dependency of the measured flow on the angle of attack of the incident current. The ideal response of a propeller is the variation of its response in proportion to the cosine of the incident flow angle (i.e., full response for flow parallel to the axle and no response to flow normal to the axle). The revolution rate of an ideal propeller sensor is proportional to the magnitude of the flow times the cosine of the angle

between the propeller axle and the flow vector. *Horizontal cosine response* refers to the sensor's response to flow in the horizontal plane, whereas *vertical cosine response* refers to the sensor's response to flow in any of the vertical planes through the sensor.

The biaxial dual-propeller current meter is designed such that, while moored in a flow field, the shaft that bears the dual propeller pairs (a total of four propellers) will remain almost vertical (see Figure 8.23). The instrument relies on the propeller sensors' cosine response—a characteristic most desirable for any CM sensor but unfortunately lacking in many of them. It has been observed (Dean, 1985) that poor cosine response can lead to rectification of wave components and therefore large errors in the measurement of mean flows. The cosine-response characteristic is particularly relevant to ocean-current sensors deployed in the wave zones because in this zone the sensor encounters a wide range of flow incident angles. Two cosine-response propeller sensors mounted at right angles to each other directly measure the components of horizontal velocity parallel to the axles of the two propellers.

The rotation of each propeller is detected by magnetodiodes—asymmetrically set so as to indicate the direction of rotation—which sense the passage of four permanent magnets embedded in an epoxy disc rotating with the propeller axle (Collar, 1993). The heading of the CM is

provided by a flux-gate compass, the output of which is sampled at a 1-Hz rate. On the production of each pulse pair by the rotation of a propeller, sine and cosine of the heading angle are added to registers storing the east-west and north-south components of the current, thus forming at the end of the sampling period a vector average of the current flow. It is quite evident that if the mean flow of magnitude U makes a horizontal angle θ with a given propeller, this propeller will sense $U\cos\theta$ and another propeller orthogonal to it will measure $U\sin\theta$. A similar pair of orthogonal propellers mounted back to back with the first set measures orthogonal components of currents from the other quadrants. This arrangement ensures that at least one sensor turns when the current comes from any angle in the horizontal plane.

Using heading signals from a suitably aligned magnetic compass within the instrument housing, the measured components are “rotated” into the conventional north-south and east-west components, averaged, and recorded. Summing the components and finding the resultant yield the vector-averaged current measurement. Because two orthogonal components of flow are directly measured, use of a direction-orienting vane is avoided for determination of flow direction. Avoidance of vane, which is an extra moving component, ensures that errors normally associated with ocean-current measurements due to imperfect response of the vane to high-frequency fluctuations are absent. Considering all these features, this current meter is popularly known as a *vector-measuring current meter* (VMCM). Preset sampling intervals between 1 and 15 minutes can be selected, the data then being written to cassette tape. The instrument is designed for inline mooring, the exterior titanium frame—from which the instrument housing is isolated—carrying the mooring tension.

The development of the biaxial dual-orthogonal propeller current meter offers an example of the way in which modeling of complex dynamic sensor response and the feedback of results from tank testing have played a central role in achieving a near-optimum design. A simple model of propeller dynamics such as that developed by Davis and Weller (1980), though neglecting interactions between propeller blades, serves to identify parameters important in determining the propeller response; it also provides insight into the nature of the compromise that must be reached in selecting the values for design parameters such as propeller pitch angle.

In steady axial flow, an ideal, frictionless propeller is accelerated until the lift-and-drag forces on its blades are perfectly balanced at a given radius along the blade, and the sensor is essentially linear. Any off-axis flow component or unsteadiness in the flow modifies the angle of attack of the blade on the fluid, thereby disturbing the dynamic balance, and hence includes contributions from the quadratic forces; a likelihood of nonlinear response then exists. Low pitch

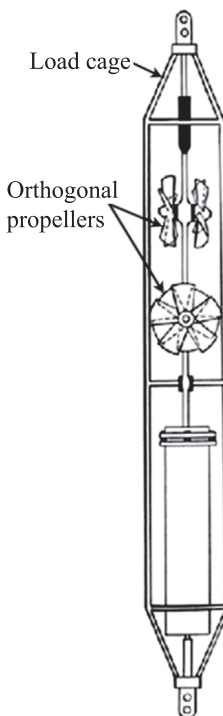


FIGURE 8.23 A biaxial dual orthogonal propeller current meter, which directly measures current vectors and is therefore known as a vector-measuring current meter (VMCM). This current meter does not have a fin. (Source: Weller and Davis, 1980.)

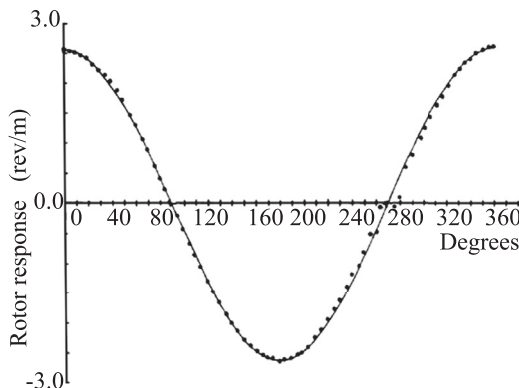


FIGURE 8.24 A typical plot of angular response of the propeller sensor attached to a VMCM, including the load cage, with flow in the horizontal plane at 25 cm/s. (Source: Weller and Davis, 1980.)

angles minimize the effects of off-axis components at the expense of increased bearing loads. However, response to unsteadiness in the axial component of the flow is also important and can be described—as for the VACM—in terms of a distance constant L , which in this case is proportional to the blade inertia and inversely proportional to the sine of the angle of attack. Excellent high-frequency response therefore demands low blade inertia and high pitch angle, and a compromise has to be sought.

Models of the instrument were made with progressively smaller spacings between the two propeller sensors and the pressure case. Tow tests of these models verified that the angular response of the sensors was degraded by placing them too close to the pressure case or to each other. The spacings chosen kept the response to flow in the horizontal plane close to cosine, whereas the response to flow with a vertical component deviated slightly from cosine due to flow disturbance by the pressure case and upstream sensor. The model included a simulation of the load cage so that any effect of flow disturbance by the rods of the load cage is included. Figure 8.24 shows a typical plot of angular response in the horizontal plane; the rms deviation of the propeller response from cosine was usually between 1.0 and 1.5 percent of the zero-degree angle of attack response. Figure 8.25 shows a typical plot of angular response to flow in a vertical plane parallel to the axle (i.e., the angle of attack of the horizontal component is kept at zero degrees, whereas the vertical angle is varied). Flow was 25 cm/s and the rms deviation of the measured response from cosine was 2.8 percent of the full-scale response.

The VMCM has been found to perform well in near-surface conditions. In combination of steady and unsteady currents, a mathematical model for the sensor predicted the possibility of “underspeeding” or underregistration of mean currents by the propeller sensor (Weller and Davis, 1980). This prediction was found to be true in actual tow-tank tests in which the instrument was subjected to combinations of steady and oscillatory flows. Results from some of the

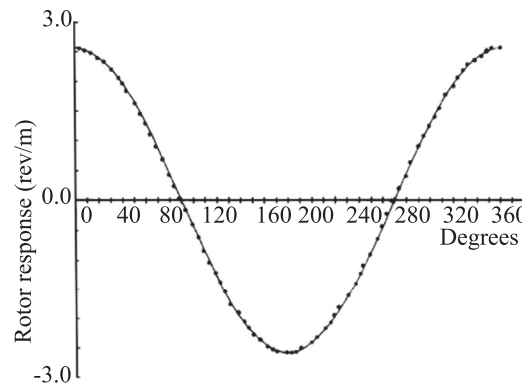


FIGURE 8.25 A typical plot of angular response to flow in a vertical plane parallel to the axle (i.e., the angle of attack of the horizontal component is kept at zero degrees whereas the vertical angle is varied). Flow was 25 cm/s, and the rms deviation of the measured response from cosine was 2.8 percent of the full-scale response. (Source: Weller and Davis, 1980.)

subsequent evaluations (Beardsley, 1987) suggest that the VMCM has the tendency to underread slightly in the presence of intense high-frequency oscillatory flows (−5 percent). It has, however, been reported that the slight underregistration error of the biaxial propeller-style current meter in such an environment is considerably small relative to the overregistration error of the Savonius rotor-style current meter under similar conditions (10–20 percent). The sensor threshold has been reported to be ~1 cm/s, i.e., the CM cannot measure currents below 1 cm/s. It has also been reported that the propeller sensors do not rectify oscillatory motion when no mean motion is present. This characteristic is a remarkable feature of the propeller sensor over Savonius rotor, which does rectify oscillatory motion in the absence of a mean current.

8.6. CALIBRATION OF CURRENT METERS

Calibration is the determination of the sensor’s response to steady-state relative motion of water past the sensor. The calibration relation is a best fit of one or more linear segments over the range of interest, expressed as an intercept and slope (Dean, 1985). Whereas laboratory calibration can be carried out at a towing-tank facility under controlled conditions, intercomparison studies are carried out in the real field under the existing natural conditions of a given water body. Laboratory calibration is usually carried out with a single current meter rigidly fastened to a trolley at one time. In a conventional procedure of CM calibration, the current meter is maintained normal to the trolley track. The towing facility includes a towed carriage that moves along two tracks built on the edges of a rectangular tank (see Figure 8.26). The carriage supports the current meter. Some tanks are provided with a shallow-water zone, which allows trouble-free mounting of the current meter on the trolley, and a deep-water zone for

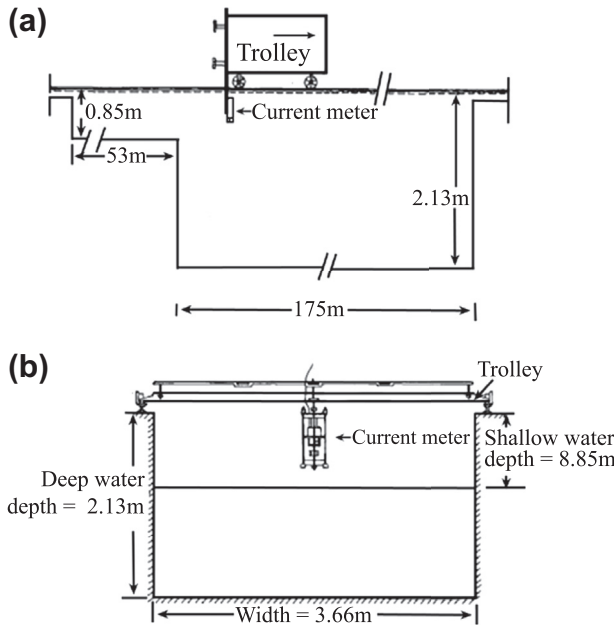


FIGURE 8.26 (a) Tow-tank and trolley facility at Central Water & Power Research Station (CWPRS) at Pune (India), used for conducting current meter calibration; (b) flow calibration setup. (Source: Joseph and Desa, 1994, ©American Meteorological Society, reprinted with permission.)

carrying out the actual calibration runs. The tow tank at the Central Water & Power Research Station (CWPRS) at Pune in India, used for conducting CM calibration runs, is part of a long channel extending from a nearby dam; therefore, the residual flow disturbances after a trolley run are rapidly damped.

The calibration setup shown in Figure 8.26b permits the CM to be moved in still water along the center of the tank with minimal flow disturbances. During calibration runs, the trolley is run at specified constant speeds, and the successive CM readings are noted, from which an average CM output value is derived. The CM is calibrated at discrete steps of towing speeds. At the end of the calibration runs at a number of discrete trolley speeds, from minimum to maximum, a calibration graph connecting a sufficiently large number of trolley speed values and the corresponding mean value of the CM outputs are plotted and the least-squares-fitted calibration equation is estimated. If the trolley speed did not maintain constant speed during a given run, the average trolley speed during that run is calculated and considered against the corresponding average value of the CM output for preparation of the calibration graph and estimation of the least-squares-fitted calibration equation.

An instrument's quality parameters such as accuracy and linearity are deduced from the least-squares-fitted calibration graph. Accuracy refers to the closeness of the instrument's output to the true value. In CM calibration, the trolley speed determined from first principles (i.e., speed defined as distance traveled in unit time interval) is taken as the true

value. The error is the difference between the instrument output and the corresponding true value, taken positively if the instrument output is greater than the true value (Doebelin, 1983). More often, accuracy is quoted as a percentage figure based on the full-scale reading of the instrument. Linearity is a specification relating to the degree of conformity of an instrument's calibration graph to the least-squares-fitted straight-line behavior. The linearity is a measure of the deviation of the calibration points from this straight line. Deviation from linearity is the difference between the instrument output and the corresponding least-squares-fitted value, taken positively if the instrument output is greater than the corresponding least-squares-fitted value (Doebelin, 1983). Linearity is usually expressed as a percentage of the full-scale reading of the instrument.

Some current meters are designed to orient into the flow irrespective of the change in current-flow direction. Gimbaled propeller current meters (e.g., Plessey current meter) and gimbaled fixed-vane type Savonius rotor current meters (e.g., Aanderaa recording current meter) are examples of such an ideal design. In such cases, the response of the flow sensor remains more or less unaffected by the changes in the direction of the current flow. However, in some designs (e.g., a free-vane system such as VACM), the CM does not orient itself in a specified direction in relation to the flow direction. If this is applicable to a given current meter, the flow sensor of which may need to be held within the supporting hardware of the current meter, the presence of the supporting hardware may give rise to differences in the CM's response with different azimuthal directions relative to the flow. In effect, the flow obstructions from the supporting hardware tend to modify the current-flow pattern in the vicinity of the flow sensor and, therefore, may affect its response to the flow field. If such a CM rotates in the azimuth for the same incident flow, the flow experienced by the flow sensor will change as the heading of the supporting hardware situated outside the sensor's periphery changes. This will introduce some errors in the current meter's output signal when the meter rotates in the azimuth.

In contrast to a fixed-vane system, the body of a free-vane system (e.g., VACM) does not have a fixed orientation with respect to the flow direction. Consequently, for the same incident flow, the flow pattern in the volume cell bounded by or surrounding the flow sensor of a free-vane system can vary during the measurement interval, resulting in corresponding variations in the flow sensor's directional sensitivity. Flow-pattern modifications imposed by a cylindrical support rod of a free-vane system can be calculated using the formula (Eskinazi, 1965):

$$V = (V_r^2 + V_\theta^2)^{1/2},$$

where V is current flow at any given point in the volume cell bounded by or surrounding the flow sensor, under the

influence of the cylindrical support rod; V_r is the flow component along the line joining a given point and the axis of the given rod; and V_θ is the flow component at this point perpendicular to V_r . Here, V_r and V_θ are given by the expressions:

$$V_r = U_o \left[\left(\frac{a_o}{r} \right)^2 - 1 \right] \cos\theta \quad (8.1)$$

$$V_\theta = U_o \left[\left(\frac{a_o}{r} \right)^2 + 1 \right] \sin\theta, \quad (8.2)$$

where U_o is the undisturbed flow approaching the cylindrical rod, a_o is the radius of the rod, r is the distance between the axis of the rod and a given point, and θ is the angle between r and the vector, U_o . The formulas for V_r and V_θ are strictly valid only for rods of infinite length and when the flow is steady. However, these calculations enable first-order estimates to be made of the flow patterns in the volume cell bounded by and in the surrounding of the flow sensor. Joseph and Desa (1994) reported calibration of a “two-support rod” current meter, which employed an Aanderaa curved-bladed Savonius rotor, at two orthogonal orientations. The calibration results supported the inferences drawn from the flow patterns estimated for the volume cell swept by the rotor blades and provided a more quantitative figure of the effective flow deviation. The results are summarized in Figure 8.27. Because flow-pattern variations at two limiting orientations have been considered, it is expected that the flow output of the meter at any other orientation will lie within the two orthogonal calibration limits. Equations 8.1 and 8.2 suggest that the asymmetries in the flow patterns in the volume cell swept by the rotor in two orthogonal orientations can be reduced either by reducing the diameter of the support rods or by increasing the pitch circle of these rods.

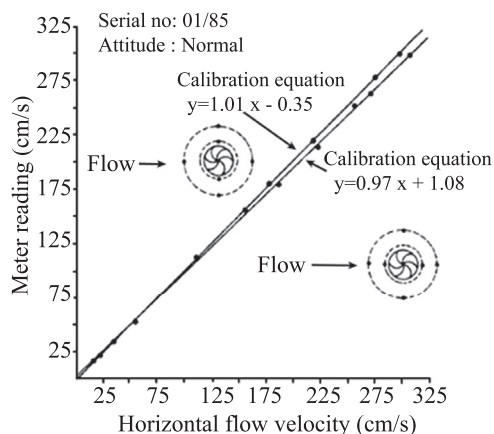


FIGURE 8.27 Calibration limits of a “two-support rod” current meter, which employed an Aanderaa curved-bladed Savonius rotor, at two orthogonal orientations. (Source: Joseph and Desa, 1994, ©American Meteorological Society, reprinted with permission.)

One method of reducing the directional sensitivity of the rotor may be the use of a sufficiently large number of support rods instead of two. Detailed tow-tank experiments by Pite (1986) have shown that the flow asymmetries can be reduced to near zero if the number of support rods surrounding the flow sensor is such that near cancellation of positive and negative asymmetries occurs.

As indicated before, in the conventional procedure of current meter calibration, the CM is maintained normal to the trolley track. However, in most cases, while the current meter is deployed in a natural flow regime, it usually undergoes tilt from the vertical. At increasing current-flow speed, the speed-dependent wakes shed from the CM’s housing are likely to generate unsteady flows in the vicinity of the flow sensor. This may cause nonlinearities in the tilt responses with increasing flow speeds. It is therefore useful to investigate the true behavior of a current meter while it is tilted from the vertical (i.e., its tilt response) at various towing speeds of interest.

Joseph and Desa (1994) conducted tilt-response experiments in a tow tank. The experimental setup used for investigation of tilt response is shown in Figure 8.28. The

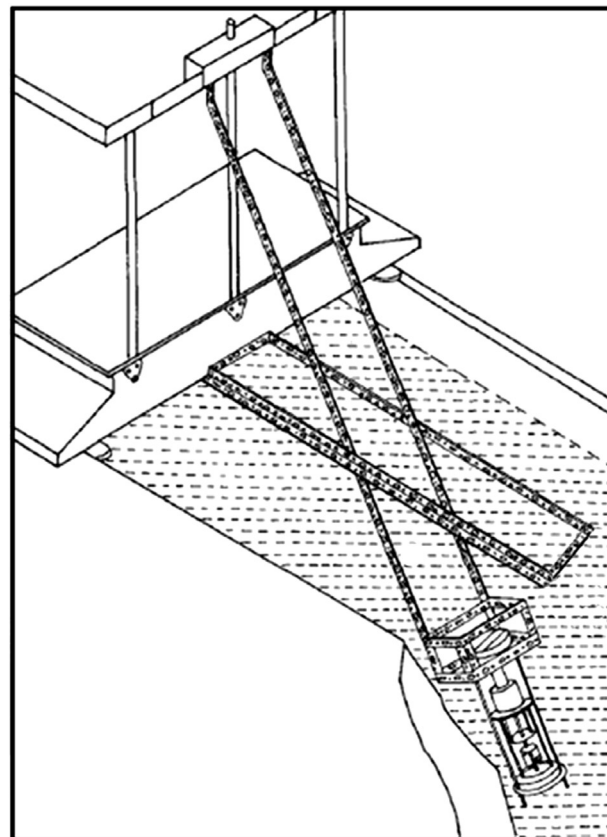


FIGURE 8.28 Experimental set-up for investigation of tilt response of a current meter. The current meter is seen attached to the tilting mechanism. (Source: Joseph and Desa, 1994, ©American Meteorological Society, reprinted with permission.)

tilting mechanism is fabricated from simple slotted angles, and the tilt angle is varied at will by simply shifting the mounting bolt from a pair of holes on the slotted angle to another pair. Because the tilting mechanism can be held above the surface of water in the tow tank, the tilting mechanism itself does not affect the flow in the vicinity of the flow sensor. In addition, because all tests can be performed on the current meter as it would be deployed in the real field, with all the hardware surrounding the flow sensor, the test results can be expected to represent the total tilt performance characteristics of the whole meter rather than that of the sensor alone. For analyzing the tilt response, for each towing speed of the current meter in its tilted position, the expected flow output of the current meter in its normal attitude can be derived from the least-squares fit of the flow calibration equation of the current meter in its normal attitude. Different flow sensors may respond differently to unsteady flows. For example, [Karweit \(1974\)](#), who conducted extensive tow-tank tests of a Savonius rotor in oscillating flows of differing frequencies, concluded that in unsteady flows the Savonius rotor may respond differently at different frequencies of the flow constituents. [Joseph and Desa \(1994\)](#) found that compared to a curved-bladed rotor, the flat-bladed rotor assembly is particularly sensitive to tilt. Its large and inconsistent deviations from cosine response have been attributed to the flow distortions caused by the semicircular cover of the rotor assembly.

The performance of a current meter in combinations of steady and oscillatory flows can be tested by adding to the tow cart a platform capable of swinging the current meter back and forth through an arc of variable period. This test set-up is shown in [Figure 8.29](#). The tow cart travels on rails at a preset speed and a motor mounted on the cart with variable-speed drive, and an arm of variable throw provides oscillatory motion by moving the current meter back and forth at the desired period and amplitude. The current meter can be rotated so that testing can be carried out for study of the current meter's azimuth response (e.g., with the axle of each sensor parallel to, at a 45° angle to, or perpendicular to the direction of tow). Shown in [Figure 8.29](#) is a prototype of the VMCM with a mock-up of the load cage so that any flow disturbance caused by the rods of the load cage will be included in the testing.

Calibration of the current meter involves not only speed performance but direction performance as well. According to [Appell et al. \(1983\)](#), a simple and inexpensive calibration facility at a field far from local magnetic influences is adequate for calibration of direction. The current meter can be placed over a graduated circle on a horizontal plane so that the vertical plane passing through the axis of the north-seeking magnetic compass points toward 0°. The current meter is then operated as is usually done in field measurements. After allowing a settling time of 30 s, the average of at least three successive readings may be noted. The current

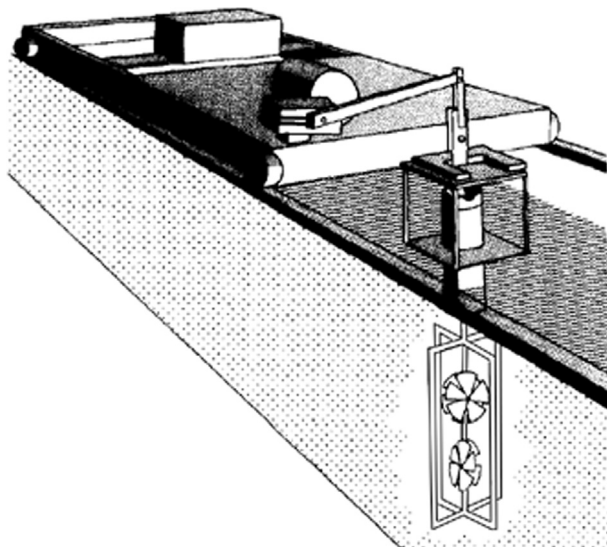


FIGURE 8.29 Test set-up used to create combinations of steady and unsteady flow. The tow cart travels on rails at a preset speed, and a motor mounted on the cart with variable speed drive and an arm of variable throw provides oscillatory motion by moving the current meter back and forth at the desired period and amplitude. Shown here is a prototype of the VMCM with a mock-up of the load cage so that any flow disturbance caused by the rods of the load cage will be included in the testing. (Source: [Weller and Davis, 1980](#).)

meter can then be slowly rotated clockwise so that the axis of the direction-orienting vane is positioned in line with the next graduation marking, separated by a discrete angular spacing (say, 10°), and an average of at least three successive readings in this new position can be recorded after allowing for adequate settling time. In this manner, readings over the entire range 0–360° in discrete steps can be recorded, with the current meter rotated in the clockwise direction. Experiments can then be repeated in the same manner with the current meter rotated in the counterclockwise direction. Based on such a direction calibration procedure, [Joseph and Desa \(1994\)](#) found that a fixed-vane CM exhibits superior direction performance compared to a free-vane CM. The comparatively poor direction performance of the free-vane system is due to the poor coupling to the “vane-follower” magnet from the external vane.

8.7. GRAPHICAL METHODS OF DISPLAYING OCEAN CURRENT MEASUREMENTS

Understanding the measured dataset is as important as the measurement itself. The first task to be carried out to retrieve meaningful information from the data (measured or modeled) is to present them in meaningful graphical formats. There are many ways of graphically presenting the water-current measurements obtained from current meters. These include time-series plots indicating the temporal variability (see [Figure 8.30](#)), stick diagrams of current

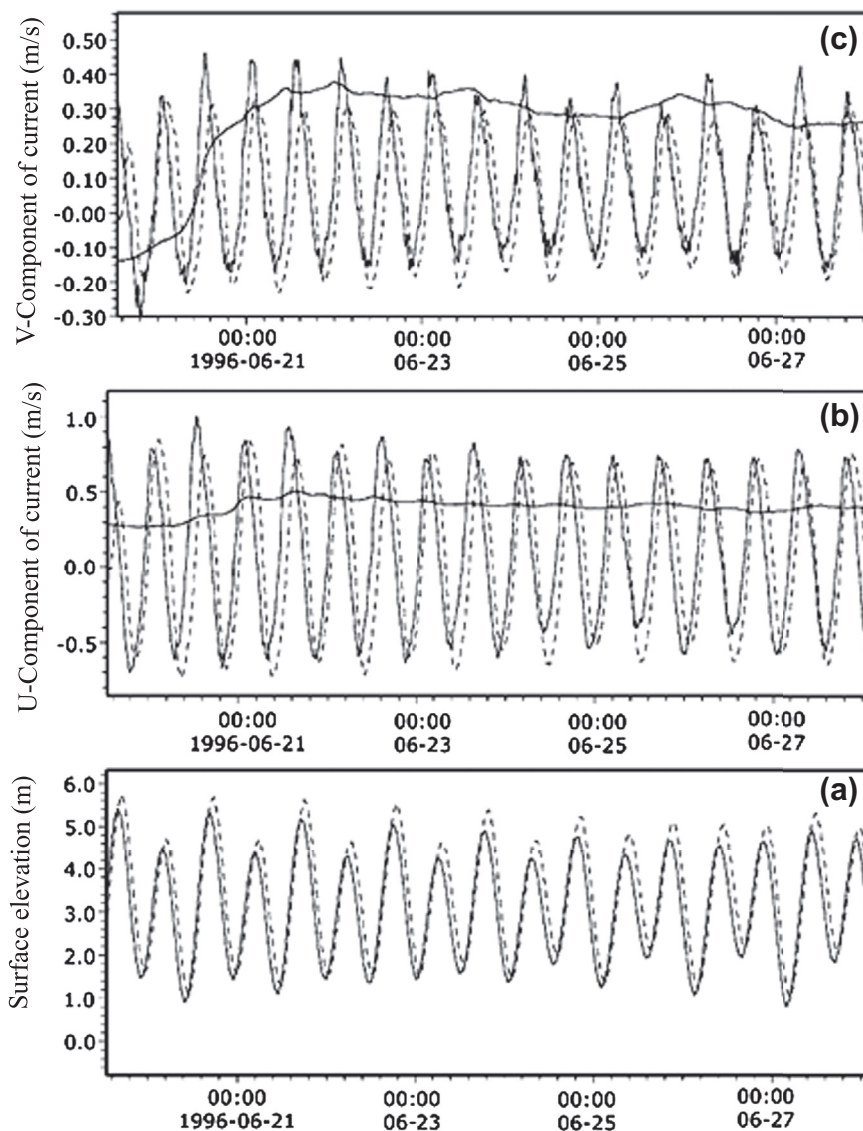


FIGURE 8.30 Time-series plots of measured and modeled current speeds and residual current during southwest monsoon conditions off Sikka in the Gulf of Kachchh in the Eastern Arabian Sea. (Source: Babu et al., 2005.)

velocity vectors that provide an indication of the temporal relationship of the current velocity vector (see Figure 8.31), rose diagrams that provide a pictorial description of the directional features of current propagation (see Figure 8.32), scatter plots (also called *dot plots*) indicating the relative spread of u and v components of currents (see Figure 8.33; see also Figure 8.22), progressive vector diagrams of currents showing the path that a fluid particle would follow (see Figure 8.34), and vertical profiles of horizontal current if current measurements are available from closely spaced depth intervals. If time-series current measurements from a geographically distant array of current meters are available, time-averaged currents for each separate location in the array can be plotted on a geographical map of the current measurements region (see Figure 8.35).

The progressive vector method takes advantage of the fact that the vertical variation in speed and direction of the current flow is usually small. If a region of fluid is imagined to be moving as a solid body, then a progressive vector plot can be viewed as a slice through the advected fluid. A standard progressive vector diagram is drawn showing the direction in which the current is flowing. For instance, if a current is flowing to the west, the point for day 2 will be drawn to the west of the point for day 1. A standard progressive vector plot can be thought of as showing the path that a fluid particle would follow. Thus, a progressive vector diagram provides an indication of the trajectory of the current.

In the case of regions of tidal dominance, plotting tidal current ellipses of various tidal constituents is an efficient

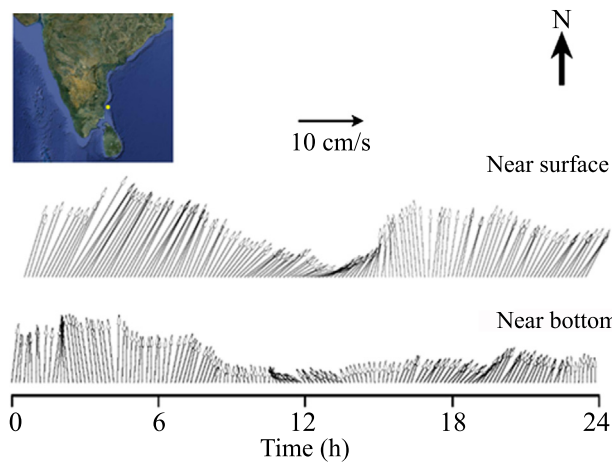


FIGURE 8.31 Stick diagrams of current vectors off Cuddalore on the southeast coast of India on May 22, 1998, at near surface and at 10 m depth. The measurement location is shown by a filled circle. (*Source: Courtesy of V. Kesavadas, P. Vethamony, and K. Sudheesh, CSIR-National Institute of Oceanography, India.*)

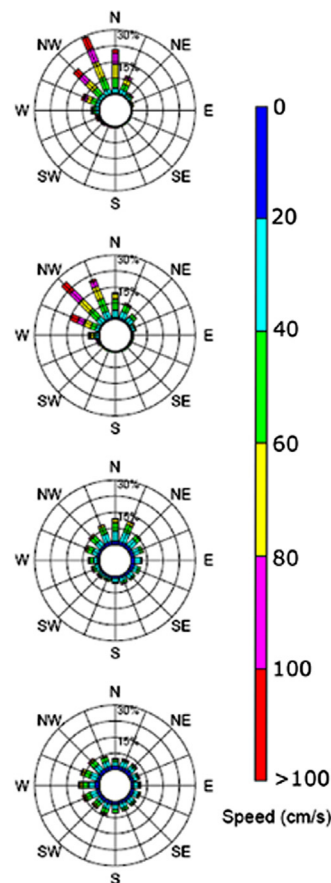


FIGURE 8.32 Rose diagrams of current velocity from five locations off Taiwan. (*Source: Liang et al., 2003.*)

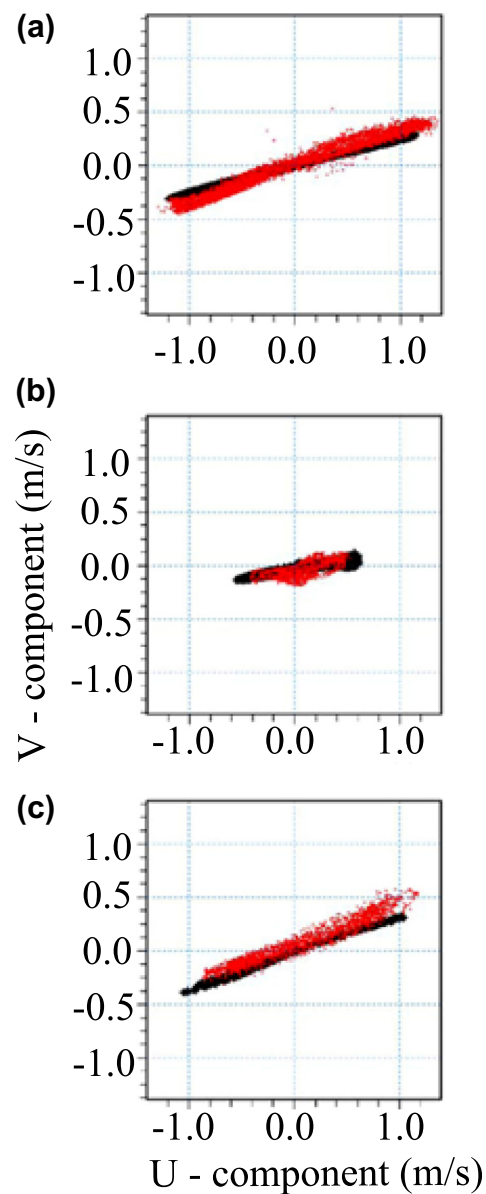


FIGURE 8.33 Scatter plots of u and v components of measured (red dots) and modeled (black dots) currents at (a) Mundra, (b) Vadinar, and (c) Sikka in the Gulf of Kachhh in the Eastern Arabian Sea. (*Source: Babu et al., 2005.*)

method of pictorially illustrating the tidal current features in a region. A harmonic analysis of the CM data yields the amplitude and phase of the east-west and north-south velocity components for each tidal constituent (Foreman, 1977). These four parameters define the tidal current ellipse that is traced out by the tip of the current vector in terms of semi-major (M) and semi-minor (m) axis, angle of inclination or ellipse orientation (Ψ), and Greenwich phase angle (ϕ). Alternatively, the tidal ellipse velocity vector can be represented by the sum of two co-rotating vectors with amplitudes of the rotary components R_+

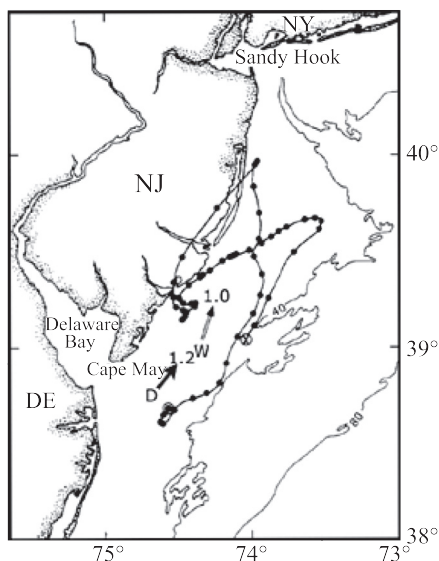


FIGURE 8.34 Progressive vector diagram of low-pass filtered surface current records during summer 1983 at a mooring on the inner continental shelf off Delaware Bay, USA. (Source: Epifanio et al., 1989.)

and R_- and phases of ϕ_+ and ϕ_- (Makinson et al., 2005). This idea is shown in Figure 8.36. There are locations in the southern Weddell Sea (e.g., along the Ronne Ice Front, Antarctica) where the M_2 rotary components, R_+ and ϕ_+ , show a strong seasonal signal that coincides with the changes in stratification at FR6 (see Figure 8.35), resulting in the amplitude of R_+ at 442 m exhibiting a two-fold increase during summer months with swings of up to

50° in ϕ_+ . The changes in ϕ_+ for the other semidiurnal tides can also change by over 40°, equivalent to 20° in ellipse orientation, which, at FR6, is typically around 55° during winter. Surprisingly, at this location, the clockwise tidal components of the semidiurnal tides (R_- and ϕ_-) and all components of the diurnal tides remain unaffected by the seasonal changes in stratification induced by intense wintertime heat loss arising from intense winds and sea-ice production. The observed specialties of the tidal ellipses in this region match observations from beneath fixed ice cover in the Arctic (Prinsenberg and Bennett, 1989) and are also predicted by the boundary layer theory (Makinson, 2002). The observed sensitivity of the anti-clockwise rotary components to changes in stratification is interpreted to be the best indicator of changes in stratification after direct observations of density variations. To identify any seasonal changes in the tidal currents, it is necessary to analyze short sections of the current meter time-series data record.

Spatially distributed tidal ellipses over a given oceanic region provide a clear indication of the nature of bathymetric and topographic influence on the tidal currents in that region (see Figure 8.37). Time-series residual currents are extracted from time-series records of current speed and direction with the use of a low-pass numerical filter (Godin, 1967) or any other convenient software packages. The resulting time series (see the residual graph in Figure 8.30) illustrates the nontidal part of the currents in a region. Vertical profiles of residual horizontal currents can also be presented graphically (see Figure 8.38).

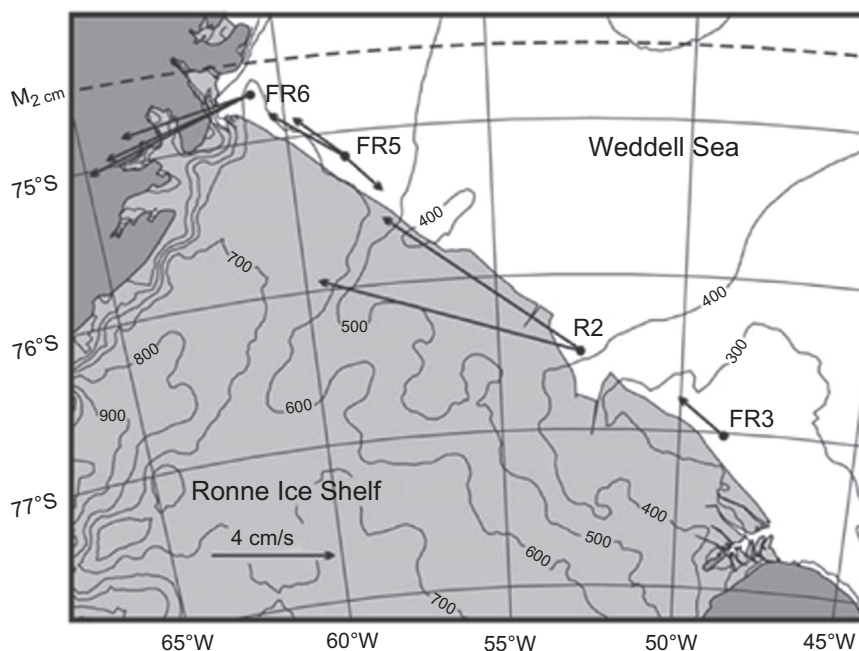


FIGURE 8.35 Time-averaged currents (indicated by arrows) at selected locations (FR3, R2, FR5, FR6) in the ice front region of the Ronne Ice Shelf in the Weddell Sea, Antarctica, plotted on a geographical map. The map shows the contours indicating the bedrock depth below sea level, with a 100-m contour interval (Vaughan et al., 1994). (Source: Makinson et al., 2005.)

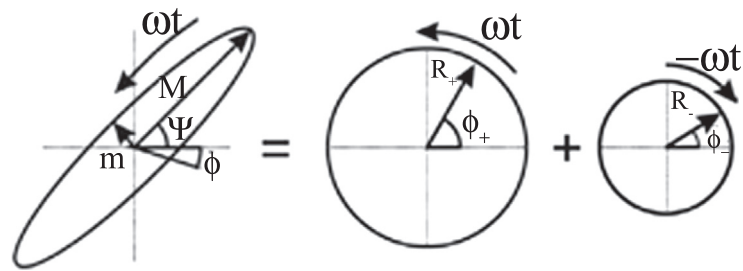


FIGURE 8.36 The basic parameters of a tidal ellipse and its two counter-rotating vectors. (Source: Makinson *et al.*, 2005.)

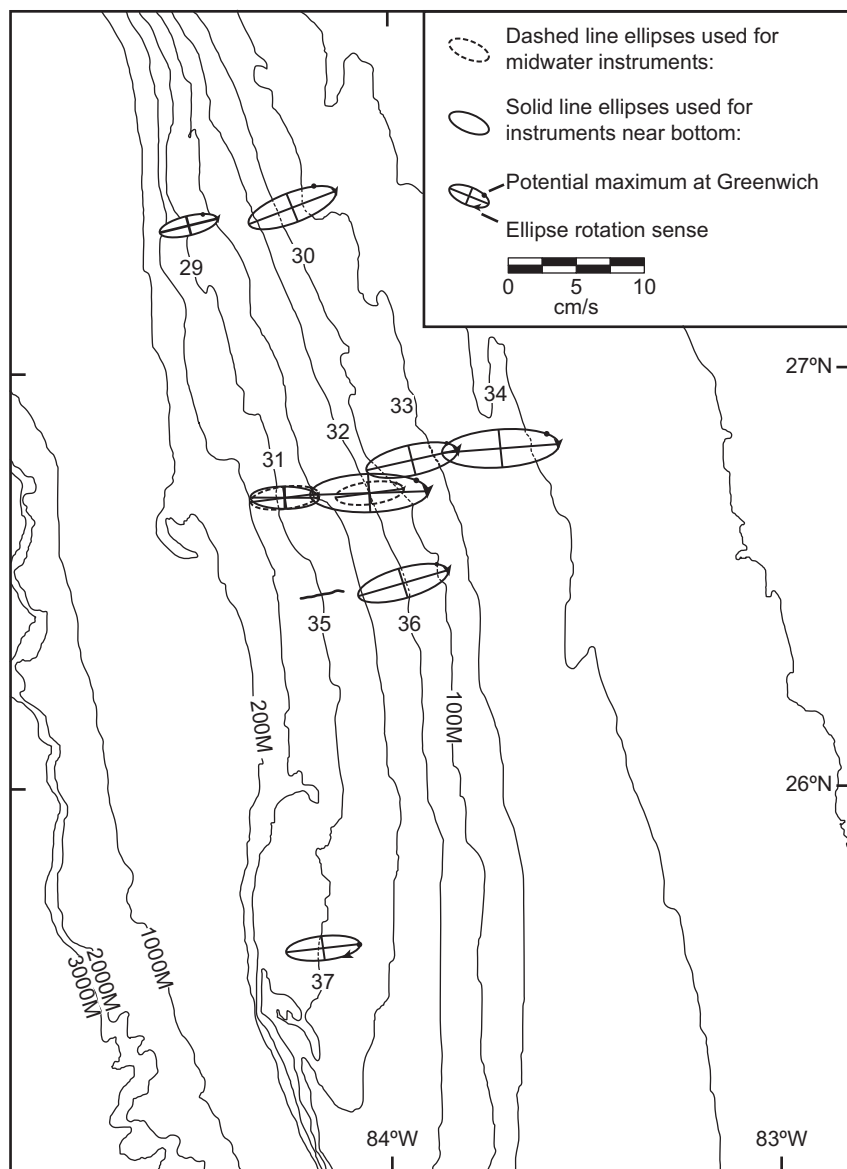


FIGURE 8.37 Spatial distribution of M_2 tidal ellipses on the West Florida Shelf. (Source: Koblinsky, 1981.)

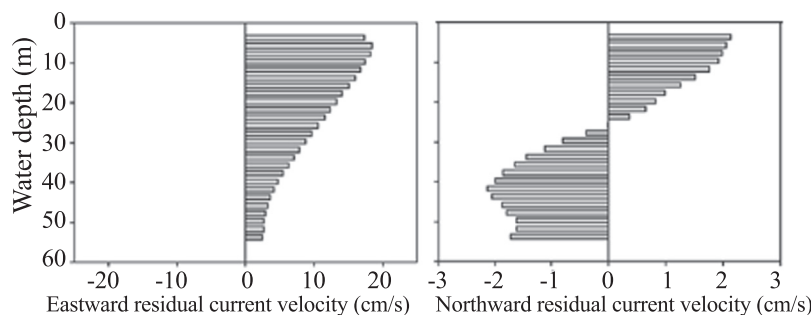


FIGURE 8.38 Vertical profile of residual current components for 24.8 h at a site in the Tachibana Bay, Japan, on July 31, 2006. (Source: Tamaki *et al.*, 2010.)

8.8. ADVANTAGES AND LIMITATIONS OF MECHANICAL SENSORS

A unique advantage of mechanical sensors is their insensitivity to changes in the surrounding environmental conditions, such as temperature, conductivity, and sediment concentration. This unique quality of mechanical sensors probably makes them the most suitable for applications in estuaries, where freshwater influx and tidal variations introduce significant salinity variations, and in locations where sediment concentration is large. (The Hugli estuary that joins to the Bay of Bengal in the Indian Ocean is an example of such a situation.) In fact, current measurements in the Hugli estuary have traditionally been carried out using CMs that incorporated mechanical sensors. Because high-frequency wave components are comparatively minimal in an estuary, the drawbacks of mechanical sensors with reference to their sensitivity to wave motions become less severe in most situations. In addition, mechanical sensors tend to be low power consumers, are durable, and are relatively cheap. Furthermore, the inherently digital nature of these sensors permits their easy interfacing to digital systems. Bidirectional propeller sensors possessing good cosine-response characteristics directly measure current vectors.

A major drawback of CMs that incorporate mechanical sensors is their lower threshold (i.e., insensitivity to very weak currents). Furthermore, their bandwidths are poor and their usefulness is limited by their inability to measure the smaller time and length scales of fluctuating turbulence components. This makes them unsuitable for fast turbulence studies. Furthermore, except for the bidirectional propeller sensors, mechanical sensors permit current measurements along only one axis. This means that they need to be oriented into the current, often using large tailfins fixed on their supporting frame. This could be a disadvantage for their application for long-term deployments in fast-reversing flows. In addition, large vanes suffer from large response times and introduce their own errors (Kenney, 1977). Current meters that incorporate mechanical sensors therefore have difficulty

measuring currents in which the mean velocities are small relative to the fluctuating currents such as those found in surface wave zones.

REFERENCES

- Aanderaa, I., 1964. A recording and telemetering instrument. NATO Subcommittee on Oceanographic Research, Technical Report No. 16, Bergen, Sweden.
- Appell, G.F., Mooney, K.A., Woodward, W.E., 1983. A framework for the laboratory testing of Eulerian current measuring devices. IEEE J. Oceanic Eng. 8, 2–8.
- Babu, M.T., Vethamony, P., Desa, E., 2005. Modeling tide-driven currents and residual eddies in the Gulf of Kachchh and their seasonal variability: A marine environmental planning perspective. Ecological Modelling 184, 299–312.
- Beardsley, R.C., 1987. A comparison of the vector-averaging current meter and New Edgerton, Germeshausen and Grier Inc. Vector-Measuring Current Meter on a surface mooring in Coastal Ocean Dynamics, Experiment I. J. Geophys. Res. 92, 1845–1859.
- Busch, N.E., Kristenson, L., 1976. Cup anemometer over-speeding. J. Applied Meteorol. 15, 1328–1332.
- Collar, P.G., 1993. A review of observational techniques and instruments for current measurements from the open sea. Report No. 304, Institute of Oceanographic Sciences, Deacon Laboratory, Wormley, Godalming, Surrey, UK.
- Davis, R.E., Weller, R.A., 1980. Propeller current sensors. In: Dobson, F., Hasse, L., Davis, R. (Eds.), Air-sea interaction: Instruments and methods. Plenum Press, New York, NY, USA, pp. 141–153.
- Dean, J.P., 1985. Problems and procedures associated with the calibration of ocean current sensors. In: Advances in underwater technology and offshore engineering, 4; Evaluation, comparison, and calibration of oceanographic instruments. Graham & Trotman, London, pp. 83–101.
- Doebelin, E.O., 1983. Generalized performance characteristics of instruments. In: Measurement systems: Application and design. McGraw-Hill, pp. 37–206.
- Epifanio, C.E., Massé, A.K., Garvine, R.W., 1989. Transport of blue crab larvae by surface currents off Delaware Bay, USA. Mar. Ecol. Prog. Ser. 54, 35–41.
- Eskinazi, S., 1965. Uniform flow around a cylinder. In: Principles of fluid mechanics. Allyn & Bacon Inc, Boston, USA, pp. 286–290.

- Fofonoff, N.P., Ercan, Y., 1967. Response characteristics of a Savonius rotor current meter. Woods Hole Oceanographic Institution Technical Report WHOI-67-33, Woods Hole, USA.
- Foreman, M.G.G., 1977. Manual for tidal currents analysis and prediction. Institute of Ocean Sciences, Patricia Bay, Sidney, BC, Canada.
- Godin, G., 1967. The analysis of current observations. Int. Hydrogr. Rev. 44, 149.
- Griffin, D.A., 1988. Mooring design to minimize Savonius rotor overspeeding due to wave action. Continental Shelf Research 8 (2), 153–158.
- Halpern, D., Pillsbury, R.D., 1976. Influence of surface waves on subsurface current measurements in shallow water. Limnology and Oceanography 21, 611–616.
- Halpern, D., Weller, R.A., Briscoe, M.G., Davis, R.E., McCullough, J.R., 1981. Intercomparison tests of moored current measurements in the upper ocean. J. Geophys. Res. 86 (C1), 419–428.
- Hansen, P., 1964. Note on the omni-directionality of the Savonius rotor current meter. J. Geophys. Res. 69, 4419.
- Hodges, G.F., 1967. The engineering for production of a recording current meter. International Hydrographic Review 44 (2), 151–168.
- Johnson, W.R., Royer, T.C., 1986. A comparison of two current meters on a surface mooring. Deep-Sea Res. 33 (8), 1127–1138.
- Joseph, A., 1991. A technique for detection of Savonius rotor oscillation. Proc. Fourth Indian Conference on Ocean Engineering, Dona Paula, Goa, India, pp. 165–168.
- Joseph, A., Desa, E., 1994. An evaluation of free-and fixed-vane flow meters with curved- and flat-bladed Savonius rotors. J. Atmos. Oceanic Technol. 11 (2), 525–533.
- Karweit, M., 1974. Response of a Savonius rotor to unsteady flow. J. Marine Res. 32, 359–364.
- Kenney, B.C., 1977. Response characteristics affecting the design and use of current direction vanes. Deep-Sea Res. 24, 289–300.
- Koblinsky, C.J., 1981. The M₂ tide on the West Florida Shelf. Deep-Sea Res. 28A (12), 1517–1532.
- Liang, W.D., Tang, T.Y., Yang, Y.J., Ko, M.T., Chuang, W.S., 2003. Upper-ocean currents around Taiwan. Deep-Sea Res. II 50, 1085–1105.
- Loder, J.W., Hamilton, J.M., 1990. Degradation of paddlewheel Aanderaa current measurements by mooring vibration in a strong tidal flow. In: Maryland, G.F., Appel Curtin, T.B. (Eds.), Proc. IEEE Fourth Working Conference on Current Measurement, April 3–5, 1990. IEEE, New York, NY, USA, pp. 107–119.
- Makinson, K., 2002. Modeling tidal current profiles and vertical mixing beneath Filchner-Ronne Ice Shelf, Antarctica. J. Phys. Oceanogr. 32 (1), 202–215.
- Makinson, K., Schroder, M., Osterhus, S., 2005. Seasonal stratification and tidal current profiles along Ronne Ice Front. FRISP Report No. 16.
- McCullough, J.R., 1975. Vector averaging current meter speed calibration and recording technique. WHOI Technical Report, WHOI-75-44.
- Paquette, R.G., 1962. Practical problems in the direct measurement of ocean currents, *Marine Sciences Instrumentation*. Instrument Society of America Vol. 2, 135–146.
- Patch, S.K., Dever, E.P., Beardsley, R.C., Lentz, S.J., 1992. Response characteristics of the VACM compass and vane follower. J. Atmos. Oceanic Technol. 9, 459–469.
- Patch, S.K., Beardsley, R.C., Lentz, S.J., 1990. A note on the response characteristics of the VACM compass. In: Maryland, G.F., Appell Curtin, T.B. (Eds.), Proc. IEEE Fourth Working Conference on Current Measurement, April 3–5, 1990. IEEE, New York, NY, USA, pp. 129–133.
- Pearson, C.A., Schumacher, J.D., Muench, R.D., 1981. Effects of wave-induced mooring noise on tidal and low-frequency current observations. Deep-Sea Res. 28A (10), 1223–1229.
- Pite, H.D., 1986. The influence of support rods on the rotation speed of Savonius rotors. J. Atmos. Oceanic Technol. 3, 487–493.
- Pollard, R.T., 1973. Interpretation of near-surface current meter observations. Deep-Sea Res. 20, 261–268.
- Prinsenberg, S.J., Bennett, E.B., 1989. Vertical variations of tidal currents in shallow land fast ice-covered regions. J. Phys. Oceanogr. 19 (9), 1268–1278.
- Ramster, J.W., Howarth, M.J., 1975. A detailed comparison of the data recorded by Aanderaa Model 4 and Plessey MO21 recording current meters moored in two shelf-sea locations, each with strong tidal currents. Deutsche Hydrographische Zeitschrift 28, 1–25.
- Saunders, P.M., 1976. Near-surface current measurements. Deep-Sea Res. 23, 249–257.
- Saunders, P.M., 1980. Overspeeding of a Savonius rotor. Deep-Sea Res. 27 A, 755–759.
- Savonius, S.J., 1931. The S-rotor and its applications. Mechanical Engineering 53, 333–338.
- Schott, F., Bedard, P., Haldenbilen, K., Lee, T., 1985. The usefulness of fairings for moored subsurface current measurements in high currents. J. Atmos. Oceanic Technol. 2, 260–263.
- Sherwin, T.J., 1988. Measurement of current speed using an Aanderaa RCM-4 current meter in the presence of surface waves. C. Shelf Res. 8 (2), 131–144.
- Tamaki, A., Mandal, S., Agata, Y., Aoki, I., Suzuki, T., Kanehara, H., Aoshima, T., Fukuda, Y., Tsukamoto, H., Yanagi, T., 2010. Complex vertical migration of larvae of the ghost shrimp, *Nihonotrypaea harmandi*, in inner shelf waters of western Kyushu, Japan, Estuarine, Coastal and Shelf Science 86, 125–136.
- Vaughan, D.G., Sievers, J., Doake, C.S.M., Grikurov, G., Hinze, H., Pozdeev, V.S., Sandhager, H., Schenke, H.W., Solheim, A., Thyssen, F., 1994. Map of subglacial and seabed topography 1:2000000 Filchner-Ronne-Schelfeis. Antarktis, Institut für Angewandte Geodäsie, Frankfurt am Main, Germany.
- Webster, F., 1972. Estimates of the coherence of ocean currents over vertical distances. Deep-Sea Res. 19, 35–44.
- Weller, R.A., Davis, R.E., 1980. A vector measuring current meter. Deep-Sea Res. 27A, 565–582.
- Woodward, M.J., 1985. An evaluation of the Aanderaa RCM-4 current meter in the wave zone. In: Proc. IEEE Conference: Ocean Engineering and the Environment. IEEE, San Diego, CA, USA. November 1985, pp. 755–762.

BIBLIOGRAPHY

- Beardsley, R.C., 1986. An inter-comparison between the VACM and new EG&G VMCM on a surface mooring. IEEE 1986, 52–62.
- Beardsley, R., Briscoe, M., Signell, R., Longworth, S., 1986. A VMCM S4 current meter intercomparison on a surface mooring in shallow water. IEEE 1986, 7–12.
- Gaul, R.D., Snodgrass, J.M., Cretzler, D.J., 1963. Some dynamical properties of the Savonius rotor current meter. In: *Marine sciences instrumentation*. Plenum Press, New York, NY, USA.

- Gould, W.J., 1973. Effects of non-linearities of current meter compasses. *Deep-Sea Res.* 20, 423.
- Halpern, D., 1986. Preliminary results of four VACM-VMCM dyads in the upper ocean of the equatorial Pacific. *IEEE* 1986, 13–19.
- Henning, B., Gandelsman, V., Cope, K., 1981. Vector-measuring current meter (VMCM). *IEEE* 1981, 522–525.
- Liang, W.D., Tang, T.Y., Yang, Y.J., Ko, M.T., Chuang, W.S., 2003. Upper-ocean currents around Taiwan. *Deep-Sea Res. II* 50, 1085–1105.
- Pingree, R.D., Maddock, L., 1985. Stokes Euler and Lagrange aspects of residual tidal transports in the English Channel and the Southern Bight of the North Sea. *J. Mar. Biol. Assoc. UK* 65, 969–982.
- Prandle, D., 1982. The vertical structure of tidal currents and other oscillatory flows. *Cont. Shelf Res.* 1, 191–207.
- Prandle, D., 1985a. On salinity regimes and the vertical structure of residual flows in narrow tidal estuaries. *Estuarine Coastal Shelf Sci.* 20, 615–635.
- Robinson, I.S., 1979. The tidal dynamics of the Irish and Celtic Seas. *Geophys. J. Roy. Astron. Soc.* 56, 159–197.
- SCOR Working Group 21, 1974. An intercomparison of some current meters. UNESCO Technical Papers in Marine Sciences. No. 17, Paris, France.
- Srinivas, K., Revichandran, C., Thottam, T.J., Maheswaran, P.A., Ashraf, T.T.M., Murukesh, N., 2003. Currents in the Cochin estuarine system (southwest coast of India) during March 2000. *Indian J. Marine Sci.* 32 (2), 123–132.
- Veth, C., Zimmerman, J.T.F., 1981. Observations of quasi-two-dimensional turbulence in tidal currents. *J. Physical Oceanogr.* 11, 1425–1430.